J. Math. Biol. (2011) 63:691–734
DOI 10.1007/s00285-010-0386-0

Mathematical Biology

Epidemic growth rate and household reproduction number in communities of households, schools and workplaces

Lorenzo Pellis · Neil M. Ferguson · Christophe Fraser

Received: 11 May 2010 / Revised: 3 November 2010 / Published online: 1 December 2010

Abstract In this paper we present a novel and coherent modelling framework for the characterisation of the real-time growth rate in SIR models of epidemic spread in populations with social structures of increasing complexity. Known results about homogeneous mixing and multitype models are included in the framework, which is then extended to models with households and models with households and schools/workplaces. Efficient methods for the exact computation of the real-time growth rate are presented for the standard SIR model with constant infection and recovery rates (Markovian case). Approximate methods are described for a large class of models with time-varying infection rates (non-Markovian case). The quality of the approximation is assessed via comparison with results from individual-based stochastic simulations. The methodology is then applied to the case of influenza in models with households and schools/workplaces, to provide an estimate of a household-to-household reproduction number and thus asses the effort required to prevent an outbreak by targeting control policies at the level of households. The results highlight the risk of underestimating such effort when the additional presence of schools/workplaces is neglected. Our framework increases the applicability of models of epidemic spread in socially structured population by linking earlier theoretical results, mainly focused on time-independent key epidemiological parameters (e.g. reproduction numbers, critical vaccination coverage, epidemic final size) to new results on the epidemic dynamics.

L. Pellis (✉) · N. M. Ferguson · C. Fraser
Medical Research Council Centre for Outbreak Analysis and Modelling,
Department of Infectious Disease Epidemiology,
Imperial College London, St. Mary's Hospital,
Norfolk Place, London W2 1PG, UK
e-mail: l.pellis05@imperial.ac.uk

Keywords Stochastic epidemic models · Real-time growth rate · Household reproduction number · Structured populations · Two levels of mixing · Epidemic dynamics

Mathematics Subject Classification (2000) 92D30

1 Introduction

Compartmental models based on systems of ordinary differential equations (ODEs) are by far the most common mathematical tools that epidemiologists use to address questions of direct practical relevance (Hethcote 2000). Their power relies on the possibility to be easily enriched by numerous features of interest (Hethcote 2000), on the solid mathematical and numerical theory of differential equations and on the availability of user-friendly numerical integration packages. However, such models rely on some unrealistic assumptions, the most fundamental of which is arguably that of random mixing (Edmunds et al. 1997; Bansal et al. 2007).

In an attempt to relax such an assumption, two main parallel streams have been evolving: the development of complex individual-based stochastic simulations (Ferguson et al. 2006; Riley 2007) and the development of models of intermediate complexity, where the effects of simple forms of heterogeneous mixing can be investigated in an analytical or semi-analytical framework. Some of these models (for example, the age-structured and the metapopulation ones; see Anderson and May 1991; Xia et al. 2004; Colizza et al. 2007), have been used in practical contexts. Others, like network models and models with an explicit social structure (e.g. households or households and workplaces) remain predominantly the focus of the most theoretically-oriented part of the epidemic modelling community (Albert and Barabási 2002; Newman 2003; Ball et al. 1997; Ball and Neal 2002; Pellis et al. 2009). The main reason for their limited use in providing quantitative answer to direct practical issues is that they are mathematically challenging and, at the same time, over-simplistic in their description of reality (Wu et al. 2006). In addition, fewer results are available about them in comparison to the standard ODE-based approach.

The present paper focuses on models in which the population is socially structured into households or households and workplaces/schools. The main aim is to enrich such theoretical models with new results to make them more useful for practical purposes.

The types of socially structured models considered here are generically referred to as models with two levels of mixing (Ball et al. 1997; Ball and Neal 2002), because a local homogeneous mixing in small environments (e.g. the household) is superimposed to a background homogeneous mixing in the population at large. When only one small environment is present, the models are usually referred to as households models (Ball and Neal 2002) and have been studied extensively in the last 15 years [starting from Becker and Dietz (1995) and the milestone of Ball et al. (1997), although preceded by an isolated pioneering work of Bartoszyński (1972)]. When two types of small environments are considered, the models usually assume that each individual belongs to both groups: for this reason, they have been referred to as overlapping

groups models (Ball and Neal 2002) or households–workplaces models (Pellis et al. 2009).

Because of the small number of individuals in each local environment, models with two levels of mixing have found fertile soil in the stochastic epidemic modelling theory and have been mostly studied in the framework of the so-called standard stochastic SIR model (Ball 1986; Andersson and Britton 2000, pp. 11–12), hereafter denoted as *sSIR model*.

However, with the exception of the Markovian case of an exponentially distributed duration of infection (Andersson and Britton 2000, pp. 34–36, 46–48) limited results concerning the epidemic dynamics are available for the sSIR model. The main reason is that the model itself is not designed to focus on the dynamics of infection spread. Most results are based on the possibility to embed a branching process approximation into the early stages of an epidemic and this approach neglects all information about the system dynamics (Andersson and Britton 2000, pp. 17, 64; Pellis et al. 2008). Nevertheless, it has proved to be extremely rewarding in terms of characterising threshold parameters, probability of epidemic extinction and critical vaccination coverage. Furthermore, important results concerning the final size distribution in the event of a large outbreak have also been obtained (Ball and Neal 2002). Such results heavily rely on some particular properties of the sSIR model, which allow also the final size to be independent of the details of the real-time dynamics of the epidemic process. Such somewhat surprising observation is motivated by an argument first proposed by Ludwig (1975) (see also Pellis et al. 2008). However, the power of this approach, i.e. the investigation of results that are independent of the times at which events occur, is in itself also a limitation, as the epidemic dynamics are often of great practical interest in themselves. They convey information about the time available to react to the spread and therefore of the effectiveness of all the control policies occurring in real-time and the impact of delays in their implementation.

The simplest piece of information concerning the epidemic dynamics is the real-time growth rate. Furthermore, it is often one of the first pieces of information readily available from data, both in the case of retrospective studies and of real-time observation of emerging outbreaks (Riley et al. 2003; Fraser et al. 2009). For this reason, the present paper focuses mostly on results concerning the real-time growth rate that characterises the initial exponentially growing phase of an epidemic. In the authors' opinion, the fact that the sSIR model is not formulated for dealing with the epidemic dynamics (the infectivity profile of an infective is kept unrealistic on purpose, to facilitate mathematical tractability, see Sect. 2.1) is probably the main reason for its limited use in practical contexts. Conversely, the deterministic time-since-infection modelling approach introduced by Kermack and McKendrick (1927) has been very useful in terms of characterising the real-time growth rate (Diekmann and Heesterbeek 2000; Fraser 2007; Roberts and Heesterbeek 2007; Wallinga and Lipsitch 2007).

Because in this paper we investigate the real-time growth rate for models where individuals mix in small groups, we need to combine the two approaches in order to retain both a stochastic modelling nature and realistic model dynamics. With this purpose, we use a stochastic model structure that has already appeared in previous studies (Fraser 2007; Goldstein et al. 2009). Earlier results (Fraser 2007; Ross et al. 2010; Goldstein et al. 2009) are reformulated into a novel and more coherent framework.

Section 2 briefly recapitulates the main assumptions of the two modelling approaches, offers a unified terminology and introduces some notation: the focus of Sects. 2.1, 2.2 and 2.3 are, respectively, the assumptions about the person-to-person infectious contact process, the social structure and possible model extensions. Section 3 offers a general framework for characterising the real-time growth rate, for models with no social structure, for the households model and for the households–workplaces model. For the same three models, Sect. 4 discusses the Markovian case of constant recovery rate and Sect. 5 discusses approximate results for the non-Markovian case. Finally, the methodology is applied in Sect. 6 and discussed in Sect. 7.

2 Basic modelling ingredients and terminology

2.1 Person-to-person infectious contact process

Throughout the paper, we refer as *infectious contact* to any contact which results in an infection whenever the first individual is infectious and the second is susceptible and we use the term *disease history* to indicate the rules according to which an individual makes infectious contacts with other individuals. The disease history is the result of a superposition of different processes (within-, between-host and in the environment; see Grassly and Fraser 2008), which are in general difficult to measure and disentangle from each other. For this reason, the form of the disease history is usually decided pragmatically by the modeller among some classical forms that make the model amenable to mathematical analysis.

Because real infections depend both on the disease history and the availability of susceptibles, they are difficult to deal with mathematically when local saturation effects due to individuals mixing in small groups are considered. Infectious contacts, instead, are independent of the state (susceptible or not) of the contacted individuals. Therefore, the models considered in the remainder of the paper will use as fundamental quantities the *infectious contact reproduction numbers* C, defined as average numbers of infectious contacts: in general the usual reproduction numbers, here denoted with the letter R, are smaller than the C's, but the two concepts coincide when saturation effects are absent, because each infectious contact results in a real infection.

The sSIR model (Andersson and Britton 2000, pp. 11–12), assumes a random disease history: upon infection, individuals experience infectious periods that are independently and identically distributed according to a random variable I, with an arbitrary distribution (we assume finite mean and variance). During the infectious period, each infective makes infectious contacts with each other selected individual according to a homogeneous Poisson process with constant rate λ. If the infectious contact occurs with a susceptible individual, he or she becomes infected. After the infectious period, the individual is immune to further infection. The Poisson processes are independent of each other and of the infectious periods. We refer to λ as the *one-to-one* infection rate.

A completely different modelling approach is the time-since-infection one originally introduced by Kermack and McKendrick (1927). Although formulated in a deterministic framework in Diekmann and Heesterbeek (2000), given the scope of

this study, we consider here the analogous stochastic formulation (as done also in Fraser 2007; Goldstein et al. 2009) and we refer to it throughout the paper as the *time-varying-infectivity model*, hereafter denoted as *TVI model*. It assumes a non-random disease history, in the sense that all individuals (or all individuals of the same type, if a multitype model is considered) have the same deterministic behaviour after infection (extensions to random disease histories are deferred to Sect. 2.3). Upon infection, an individual is assumed to make infectious contacts with other randomly selected individuals according to a Poisson process with time-varying infection rate described by a non-negative function (or, more generally, a distribution) $\beta(\tau)$, identical for each infective, where τ represents the time elapsed since the infection of the individual ($\beta(\tau) = 0$, for $\tau < 0$). The *infectivity profile* $\beta(\tau)$ is often factorised as $\beta(\tau) = C\omega(\tau)$, where $C = \int_0^{+\infty} \beta(\tau)\mathrm{d}\tau$ represents the individual's total infectivity (assumed to be finite) and $\omega(\tau)$ represents the distribution of times since infection at which an infective makes infectious contacts with other individuals. We refer to it as the *infectious contact time distribution* or, as in Goldstein et al. (2009), as the *infectious contact interval distribution*.

Note that the TVI model is parameterised in terms of a *one-to-all* infection rate β. Comparison between the models in a population of size n can be achieve by relating β and λ (whether they are constant or time-dependent) as $\beta = (n-1)\lambda$. Because recent empirical evidence (Cauchemez et al. 2004, 2009) rejects the density-dependent contact rate hypothesis even in small groups like households, we make the assumption that a frequency-dependent contact rate occurs in every mixing group throughout the paper. Therefore, it is convenient to parameterise both models in terms of the one-to-all contact rates β, so that, for increasing group sizes, the one-to-one rate λ changes, but β and therefore the average number C of infectious contacts an individual makes remain constant.

Finally, note that both models paradigms satisfy the following assumption:

(A.1) *The infectious behaviour of an individual is independent of the time of infection and the identity of the infector.*

This fundamental assumption implies that, even if random, the behaviour of an individual upon infection can be drawn before the epidemic starts. In particular, we exclude correlations between the behaviour of an infector and the behaviour of the infectee. This is the case of many, but not all, models appearing in the literature (an example of model that violates this assumption is the so-called "infector-dependent-severity model": see e.g. Kendall and Saunders 1983; Svensson and Scalia-Tomba 2001; Ball and Britton 2007). This assumption has some limitations (see, for example, Pellis et al. 2008) and is discussed further in Appendix A because we heavily rely on it for decomposing the infectivity profile of households in terms of the infectivity profile of individuals.

2.2 Social structure

Because we are interested in studying the real-time growth rate, we consider the limit of an infinite and fully susceptible population and we focus on the *early phase* of the epidemic, i.e. the time window when an already established epidemic is characterised

by an exponential growth in the number of cases. Therefore, it is implicitly assumed that $R_0 > 1$ and the epidemic has not gone extinct by random chance. A formal argument requires considering the asymptotic behaviour of a sequence of epidemics in populations of size $N \to +\infty$. This approach allows a well defined distinction between small and large epidemic: denoting by Z the final number of individuals infected during an epidemic, we define the epidemic as *small* if $z = Z/N \to 0$ as $N \to +\infty$, i.e. if the epidemic went extinct after only a finite number of cases was infected. If a positive fraction z of the population is infected, the epidemic will be called *large*.

As a notational convention, throughout the paper we refer to an unstructured population using variables with no subscript and we denote the basic reproduction number as R_0. In the presence of structure, we use small case subscripts to refer to quantities involved in processes at the individual level (in the community or within households or workplaces). Capitalised subscripts refer instead to quantities involved in processes at the scale of local structures (households or workplaces).

In the households model with TVI disease history, an individual makes infectious contacts with other individuals (one-to-all) in the same household according to a Poisson process with a time-varying infection rate $\beta_h(\tau)$, where τ represents the time elapsed since the infection of the individual. We define as $C_h = \int_0^{+\infty} \beta_h(\tau)\mathrm{d}\tau$ the within-household infectious contact reproduction number, i.e. the average number of household infectious contacts, and we to factorise $\beta_h(\tau)$ as $\beta_h(\tau) = C_h\omega_h(\tau)$ where $\omega_h(\tau)$ is the *within-household infectious contact time distribution*, i.e. the distribution, normalised such that $\int_0^{+\infty} \omega_h(\tau)\mathrm{d}\tau = 1$, of the times at which an infective makes infectious contacts towards other households members. In addition, the same individual makes infectious contacts with other randomly selected individuals in the population (one-to-all) according to a Poisson process with rate $\beta_g(\tau)$ (the subscript g stands for *global*). Again, we factorise $\beta_g(\tau)$ as $\beta_g(\tau) = C_g\omega_g(\tau)$, where C_g is the global infectious contact reproduction number and the global infectious contact time distribution $\omega_g(\tau)$ satisfies $\int_0^{+\infty} \omega_g(\tau)\mathrm{d}\tau = 1$.

Note that, unlike most other similar studies (Fraser 2007; Goldstein et al. 2009), the present methodology allows for the infectious contact interval distribution to be different in the household and outside. Such a feature may be of interest if one wants to model the fact that infected individuals are likely to mix freely outside their households until they start feeling sick, at which point they tend to spend most of their time at home, thus posing the other households members at a higher risk of getting infected.

As the population size N tends to infinity (while keeping fixed the household size distribution) and during the early phase of the epidemic, it is well established (e.g. see Ball et al. 1997; Ball and Neal 2002; Andersson and Britton 2000; Fraser 2007; Goldstein et al. 2009) that all global infectious contacts result in global infections and start new household epidemics, which develop independently of one another through household infections only. Because all global infectious contacts result in an infection, the global reproduction number R_g will be used instead of C_g. The distribution $\omega_g(\tau)$ now represents what is usually referred to in the literature as the *generation time distribution*. In this context, we define as *susceptible* a household with all susceptible members, *infected* a household with at least one infective member and *immune* a households in which the household epidemic has finished. (Note that once the early

phase is over, then the infection can be reintroduced again in what we call here immune households.) Since all infectives in a household can infect other individuals via global infectious contacts, and each of these belongs almost surely to a different household, the process can be interpreted as a household infecting other households. A reproduction number for households is usually referred to as R_* and satisfies the usual threshold condition: large epidemics can occur only if $R_* > 1$. With the exception of the primary case in a household, we refer to all other cases infected in a household epidemic as *secondary cases*, even if they have not been infected directly by the primary case. In this perspective, all secondary cases are thought of as deriving from the primary case, and no secondary case is seen as responsible for other infections in the household. Denoting by μ_H the average number of secondary cases of an epidemic in the household of a randomly selected individual, we have the Wald's identity for epidemics (see Ball 1986; Andersson and Britton 2000, p. 15; Pellis et al. 2009):

$$R_* = R_g(1 + \mu_H).$$

The households–workplaces model is a natural extension to the households model. In addition to households and global infectious contacts, the workplace one-to-all infectious contact rate is denoted by $\beta_w(\tau) = C_w\omega_w(\tau)$, where ω_w has integral 1. We refer to both households and workplace infectious contacts as *local infectious contacts*, as opposed to global ones.

Following Pellis et al. (2009) we assume that:

(A.2) *The network connecting households and workplaces is a bipartite random network.*

In other words, we assume for simplicity that individuals choose their workplace at random. Note that this is usually not the case in realistic populations, for example because siblings are more likely attend the same school. Under this simplifying assumption, however, as the population size $N \to +\infty$, finite loops in this network appear with vanishing probability. Therefore, a chain of epidemics via local infections only infects new local environments (households, workplaces, households again and so on) in a "tree-like" process. Ball and Neal (2008) refer to the set of individuals infected in this chain of only local infections as a *clump*. A slightly different perspective appears in Pellis et al. (2009) and is the one briefly summarised here (see the original paper for details): households are seen as infecting other households globally (G), i.e. via global infections, or locally (L), i.e. through workplace epidemics. The model so obtained is a two-type model for households, with a next generation matrix $K_H = (R_{ij}), i, j \in \{G, L\}$, where R_{ij} represents the average number of households infected via mode i by a household that was itself infected via mode j. In addition to R_g and μ_H as defined before, denote by μ_W the average number of initial susceptibles who are finally infected in a workplace epidemic (workplace secondary cases, in our terminology). Then we have: $R_{GG} = R_{GL} = R_g(1 + \mu_H)$, $R_{LG} = \mu_W(1 + \mu_H)$ (the primary case in the household epidemic is infected through a global infectious contact and can trigger an epidemic also in his or her workplace) and $R_{LL} = \mu_W\mu_H$ (the primary case in the household was infected in a workplaces epidemic and is considered a secondary case in that epidemic, so is not interpreted as infecting anyone

else back in the workplace). A household reproduction number R_H is then defined as the dominant eigenvalue of K_H:

$$R_H = \rho(K_H) = \rho\begin{pmatrix} R_{LL} & R_{LG} \\ R_{GL} & R_{GG} \end{pmatrix}, \tag{1}$$

where $\rho(\cdot)$ is the spectral radius of the square matrix $\cdot$. The reproduction number R_H satisfies the usual threshold condition around 1.

2.3 Model extensions

Whatever the social structure assumed, a possible extension of the TVI model is obtained when a random TVI disease history is considered, as explained here. We refer to it as the *random TVI model*. In this case, we assume that all individuals have the same susceptibility and a random infectivity profile $B(\tau)$ drawn, independently for each infective, from a suitable set $\mathscr{B}$ with probability distribution denoted by the measure ζ (i.e. $\int_{\mathscr{B}} \mathrm{d}\zeta(B) = 1$). ($B(\tau)$ could be, for example, the outcome of a within-host random process modelling the competition between the pathogen and the host's immune system.) We denote by

$$\beta(\tau) = \int_{\mathscr{B}} B(\tau)\mathrm{d}\zeta(B)$$

the average infectivity profile of an individual.

This extension of the TVI model allows the inclusion of the sSIR model in this formalism. The classical example is given by the Markovian SIR model. In this case, $B(\tau) = \beta\,\Theta_{[0,I]}(\tau)$, where β represents the constant one-to-all infection rate, $\Theta_{[l_1,l_2]}$ represents the Heaviside function, defined as

$$\Theta_{[l_1,l_2]}(x) = \begin{cases} 1 & \text{when } l_1 \le x \le l_2, \\ 0 & \text{otherwise,} \end{cases}$$

and the length of the infectious period I is drawn from an exponential distribution with parameter ν. In this case, $\mathscr{B} = \{B(\tau) = B_I(\tau) = \beta\,\Theta_{[0,I]}(\tau),\, I \in \mathbb{R}^+\}$ and $\mathrm{d}\zeta(B_I) = \nu \mathrm{e}^{-\nu I}\mathrm{d}I$.

Characterising the real-time growth rate for random TVI model is straightforward when there is no social structure. However, in the presence of local saturation effects, exact results seem to be possible only in the particular case of Markovian processes, i.e. in the analytical framework of continuous-time Markov chains (CTMCs). In Sect. 4, only the simplest possible Markovian process, with no latent period and a single infectious stage, is discussed. CTMCs with multiple stages of infection, leading to a Γ-distributed duration of infection, have been included in households models, for example, in Ross et al. (2010).

In the case of non-Markovian processes, approximate but explicit results can be obtained if we introduce a further assumption:

(A.3) *The random total infectivity and the random infectious contact time distribution within each infective (in every environment) are independent of each other.*

This assumption is rather strong and is needed to separate the random process describing how many infectious contacts an infective makes and the process describing the times when they are made. In other words, similarly to before, this assumption allows the factorisation of the average infectivity profiles as $\beta_g(\tau) = R_g\omega_g(\tau)$, $\beta_h(\tau) = C_h\omega_h(\tau)$ and $\beta_w(\tau) = C_w\omega_w(\tau)$ in the community, household and workplace respectively. Here, R_g, C_h and C_w represent the average numbers of infections contacts made in each environment and the ω's, normalised to have integral 1, represent the (pointwise) averages of the infectious contact time distributions. Note that Assumption (A.3) is required only to make further analytical progress in the non-Markovian case. The general theory of Sect. 3 does not invoke it. In fact, the general theory applies also to the Markovian case discussed in Sect. 4, where this assumption is not met since individuals with longer infectious periods have a larger total infectivity. A particular case (considered, for example, in Fraser et al. 2009) when this assumption is satisfied is when, in each environment, ω is the same for every individual, but the total infectivity is allowed to vary between individuals. Some examples of computations involving the random TVI disease history under Assumption (A.3) can be found at the end of Appendix E.

The second possible model extension is towards multitype models. This requires distinguishing households and workplaces according to their composition, i.e. according to how many members of each type they have. Because such a generalisation is straightforward but cumbersome, for the sake of simplicity, throughout the paper we assume individuals of a single type only.

However, we consider the case of households and workplaces of different sizes. For this reason, we still need to recall how to compute the real-time growth rate for a multitype model with no social structure, as this model applies directly to the interaction of local structures of variable size, observed at the level of households.

3 Computation of the real-time growth rate

3.1 Models with no local saturation

Consider the model with non-random TVI disease history in a large, single-type, homogeneously mixing population. Following Diekmann and Heesterbeek (2000, p. 103), the real-time growth rate r, conditional on a large epidemic taking place, is given by the implicit solution of the Lotka–Euler equation

$$\int_0^{+\infty} \beta(\tau)e^{-r\tau}\mathrm{d}\tau = 1, \tag{2}$$

where the left-hand side is the Laplace transform of β calculated in r, $L_\beta(r)$. The solution of (2) exists and is unique, because $L_\beta(r)$ is a monotonically decreasing function of r, with $\lim_{r\to+\infty} L_\beta(r) = 0$ and $L_\beta(0) = R_0 > 1$.

The result can be readily extended to the case of a single-type model with random disease history, thanks to the fact that the Laplace transform L_B is linear in B. The equation for the real-time growth rate r is:

$$\begin{aligned} 1 &= \int_{\mathscr{B}} \left(\int_0^{+\infty} B(\tau) \mathrm{e}^{-r\tau} \mathrm{d}\tau \right) \mathrm{d}\zeta(B) \\ &= \int_0^{+\infty} \beta(\tau) e^{-r\tau} \mathrm{d}\tau, \end{aligned}$$

where $\beta(\tau) = \int_{\mathscr{B}} B(\tau) \mathrm{d}\zeta(B)$ represents the average infectivity profile of an individual. (We assume all the regularity conditions needed for the integral exchange and the existence of an average profile β.)

As an example, recall that, in the case of the Markovian SIR model, $B(\tau) = \beta\, \Theta_{[0,I]}(\tau)$ and $\mathrm{d}\zeta(B_I) = \nu \mathrm{e}^{-\nu I} \mathrm{d}I$. Using the fact that $\Theta_{[0,I]}(\tau) = \Theta_{[\tau,+\infty)}(I)$, we have

$$\begin{aligned} \beta(\tau) &= \int_0^{+\infty} \beta\, \Theta_{[0,I]}(\tau) \nu e^{-\nu I} \mathrm{d}I \\ &= \int_\tau^{+\infty} \beta\, \nu e^{-\nu I} \mathrm{d}I \\ &= \beta\, e^{-\nu\tau}. \end{aligned}$$

Solving Eq. (2) for r gives the usual $r = \beta - \nu$.

When a random susceptibility is considered in addition to the random infectivity, care needs to be taken in how the average infectivity of an individual is defined, because more susceptible individuals are more likely to be infected. If susceptibility and infectivity of a single individual are represented by the random quantities A (a scalar) and $B(\tau)$ (a distribution), respectively, then the average infectivity profile at each time τ is given by the weighted average $\beta(\tau) = \mathbb{E}[AB(\tau)]$ (weighted to correctly overrepresent more susceptible individuals). This is in general different from the product of the averages when the two random quantities are correlated.

When a multitype model is considered, with susceptibility and disease history assumed to be non-random for each type, it is necessary to define the operator (see Diekmann and Heesterbeek 2000, p. 103)

$$K_r = \left(\int_0^{+\infty} \beta_{ij}(\tau) e^{-r\tau} \mathrm{d}\tau \right) = \left(L_{\beta_{ij}}(r) \right),$$

where L denotes the Laplace transform applied to its subscript and $\beta_{ij}(\tau)$ represents the average infectivity profile from a single infective of type j towards all individuals of type i, which takes into account, as well as the particular mixing patterns, also the infectivity of type j, the susceptibility of type i, and the proportion of individuals of type i in the population. Conditioned on K_r being irreducible, the real-time growth rate r is therefore obtained as the solution of the implicit equation

$$\rho(K_r) = 1, \tag{3}$$

where, the left-hand side $\rho(\cdot)$ is the dominant eigenvalue of the matrix $\cdot$. The solution exists and is unique because $\rho(K_r)$ is monotonic in r with $\lim_{r\to+\infty} K_r = 0$ and $\rho(K_0) = R_0 > 1$ (see Diekmann and Heesterbeek 2000, p. 104).

A particularly simple case, where the distributions β_{ij} can be factorised in the product of the two separate contributions of the type j of the infector and the type i of the infectee, is usually referred to as *separable mixing* (Diekmann and Heesterbeek 2000, p. 80). This is the case, for example, when $\beta_{ij}(\tau) = h_i a_i b_j(\tau)$, where h_i is the fraction of individuals of type i, a_i is their susceptibility and $b_j(\tau)$ is the infectivity profile of an infective of type j. The product $\alpha_i = a_i h_i$ will also be referred to as the *susceptibility-availability* of individuals of type i. In this case, similarly to the case of a single type model with random susceptibility and infectivity, the infectivity profile of an average individual is the result of a weighted average of the infectivity $b_i(\tau)$ of different types i, with weights proportional to susceptibility-availability α_i of each type.

The analysis becomes more complex when randomness is superimposed on the multitype structure (*multitype randomised model*: see Neal 2006). However, at least in the case of separable mixing, it is still sufficient to average across the distribution of disease histories for each type j, with weights given by the distribution of susceptibilities, to recover the same condition above. If separable mixing cannot be assumed for the multitype model, then the analysis is even more complex. It is still reasonable to expect that the system can reduce to that of a multitype model, by averaging across each type, although a formal proof would be needed. A particular case of this type concerning the model with households and workplaces is considered in Appendix C.

3.2 Households model

Consider a households model with random TVI disease history where (A.1) holds, and assume initially that all households of the same size n_H. When a household is infected, a stochastic epidemic (driven only by households infections) spreads through it. Let $U \in \mathscr{U}$ be a parameter vector that fully describes the household epidemic and let ζ be the measure over $\mathscr{U}$ associated with the probability density of occurrence of each possible household epidemic. Even if the disease history of individuals were non-random, the disease history of a household is random and is denoted by $B_H^U(\tau_H)$, where τ_H represents the time since the infection of the household. However, using the same arguments as before (see also Fraser 2007), the real-time growth rate for households, r_H, is determined by the average household infectivity $\beta_H(\tau_H) = \int_{\mathscr{U}} B_H^U(\tau_H) \mathrm{d}\zeta(U)$ as the solution of

$$L_{\beta_H}(r_H) = 1, \tag{4}$$

where L denotes the Laplace transform of its subscript.

It is proved in Appendix A that the average household infectivity profile can be decomposed in

$$\beta_H(\tau_H) = \beta_g(\tau_H) + \beta_g * \gamma_H(\tau_H), \tag{5}$$

where β_g is the average global infectivity profile, $*$ denotes the convolution operation and γ_H represents the average rate at which new infected cases appear in the household, with

$$\int_0^{+\infty} \gamma_H(\tau_H)\mathrm{d}\tau_H = \mu_H.$$

The first term refers to the global infections generated by the household primary case, while the second is the contribution to global infections given by all the secondary cases.

Note that the real-time growth rate r_H refers to households, while one is usually interested in the rate at which the number of infected cases grows. However, we have the following.

Theorem 1 *Let r be the real-time growth rate for the exponential growth of the number of infected individuals and let r_H be the real-time growth rate for the exponential growth of the number of infected households. Then $r = r_H$.*

A formal proof of this results is reported in Appendix B, but an intuitive argument for it could be the following: if $H(t)$ is the prevalence of households at time t, then the number of infected individuals $Y(t)$ is roughly given by $(1 + \mu_H)H(t)$, and if $H(t) \propto \mathrm{e}^{rt}$, then $Y(t)$ shares the same growth rate.

In the case of households of different sizes, the model can be seen as a multitype randomised model with separable mixing, where the size of each household determines its type. In fact, if h_n represents the fraction of households of size n, a household of size n has probability $\pi_n = nh_n \big/ \sum_n nh_n$ of being infected and, after infection, exerts a random time-varying infectivity $\beta_H^{U_n}(\tau_H)$ with average, say, $\beta_H^{(n)}(\tau_H)$. The overall real-time growth rate is given again by Eq. (4), where now $\beta_H(\tau_H) = \sum_n \pi_n \beta_H^{(n)}(\tau_H)$. The distribution π_n is often referred to as the *size-biased distribution* (e.g. Ball et al. 1997).

3.3 Households–workplaces model

Theorem 1 suggests that, during the exponentially growing phase, the real-time growth rate of all structures (with finite average size) is the same. Therefore, it is sufficient to calculate the easiest one to obtain: we focus on the one for households.

As a side remark, note that when clumps (see Ball and Neal 2002 or Sect. 2.2) have finite average size, the same real-time growth rate can also be thought of as referring to clumps. However, the usefulness of this interpretation is limited, given that the time a clump requires to form can in general be comparable to that of the entire epidemic. Therefore, in realistic settings, any exponentially growing phase could be too short to observe enough clumps to motivate a deterministic approximation.

Assume, for the time being that all households have the same size n_H and all workplaces have size n_W. Distinguishing households according to how their primary case was infected (i.e. globally, or locally through a workplace), we obtain a two-type randomised model. In addition to τ_H and $\gamma_H(\tau_H)$ as defined for the households model, denote by τ_W the time since the infection of a workplace and by $\gamma_W(\tau_W)$ the average rate at which new cases appear in a workplace epidemic, with

$$\int_0^{+\infty} \gamma_W(\tau_W)\mathrm{d}\tau_W = \mu_W.$$

The average rate at which a household infected locally infects another household locally is given by $\beta_{LL}(\tau_H) = \gamma_W * \gamma_H(\tau_H)$ (recall that the primary case is not counted actively when the local structure is infected locally; see Sect. 2.2 or Pellis et al. 2009). Analogously the average rate at which a household infected globally infects other households locally is given by $\beta_{LG}(\tau_H) = \gamma_W(\tau_H) + \gamma_W * \gamma_H(\tau_H)$. The other two cases are: $\beta_{GG}(\tau_H) = \beta_{GL} = \beta_g(\tau_H) + \beta_g * \gamma_H(\tau_H)$.

The real-time growth rate r is obtained by imposing that the operator

$$K_r = \begin{pmatrix} \int_0^{+\infty} \beta_{LL}(\tau_H)e^{-r\tau_H}\mathrm{d}\tau_H & \int_0^{+\infty} \beta_{LG}(\tau_H)e^{-r\tau_H}\mathrm{d}\tau_H \\ \int_0^{+\infty} \beta_{GL}(\tau_H)e^{-r\tau_H}\mathrm{d}\tau_H & \int_0^{+\infty} \beta_{GG}(\tau_H)e^{-r\tau_H}\mathrm{d}\tau_H \end{pmatrix} \tag{6}$$

has dominant eigenvalue equal to 1. Because we are observing a large epidemic,

$$\rho\left(K_0\right) = \rho\begin{pmatrix} R_{LL} & R_{LG} \\ R_{GG} & R_{GG} \end{pmatrix} = R_H > 1.$$

Since $\lim_{r\to+\infty} \rho(K_r) = 0$ and $\rho(K_r)$ is a monotonic function of r, the equation

$$\rho(K_r) = 1 \tag{7}$$

admits a unique solution.

When households and workplaces have variable sizes, the computation of r reduces again to that of a two-type model, although a formal argument for it requires a more cumbersome notation and is reported in Appendix C. The key points is that the size of one structure is independent of the size of the other because of the bipartite random network assumption (see Sect. 2.2).

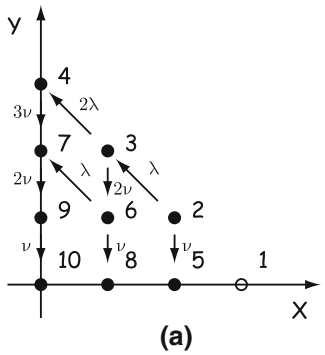

Event	State transition	Transition rate
Infection	$(i,j) \to (i-1, j+1)$	$\frac{\beta ij}{n-1} = \lambda ij$
Recovery	$(i,j) \to (i, j-1)$	νj

Fig. 1 **a** Graphical representation of all possible states for an *SIR* epidemic in a population of size $n = 3$. States are also labelled sequentially with index $k = 1, \ldots, 10$, showing how κ_3 is defined. **b** All possible transitions and their rate of occurrence

4 Exact results for the Markovian case

4.1 Exact epidemic dynamics in a small population

Consider the CTMC describing an epidemic in a small population of size n and assume that individuals are all identical, that the total population is constant and that an individual can be susceptible (X), infected (Y) or recovered (Z). The state space Ω of the system is given by all the pairs (X, Y) where $X \geq 0, Y \geq 0$ and $X + Y \leq n$: then $Z = n - X - Y$.

Figure 1 offers a schematic representation for $n = 3$ and all the possible transitions, where $\lambda = \beta/(n-1)$ is the one-to-one infectious contact rate and ν the constant recovery rate.

The generator matrix Q can be written explicitly once we specify a map κ_n that associates the pair (i, j) to a single index k, such that the state $\omega_k \in \Omega$ represents the epidemic state $(X, Y) = (i, j)$ (an example is given in Fig. 1). The element q_{hk} of the generator matrix represents the rate of progression from state ω_h to ω_k, i.e. form state $(i_h, j_h) = \kappa_n^{-1}(h)$ to state $(i_k, j_k) = \kappa_n^{-1}(k)$. The corresponding element $p_{hk}(t)$ of $P(t) = e^{tQ}$ represents the probability that the system is in state (i_k, j_k) if it was in state $(i_h, j_h)t$ units of time ago or, equivalently, that the system is in state (i_k, j_k) at time t if it started from state (i_h, j_h).

Another quantity of interest is the matrix

$$M(t) = \int_0^t e^{\sigma Q} \mathrm{d}\sigma, \tag{8}$$

where the integral is taken componentwise. Each element $m_{hk}(t)$ of $M(t)$ represents the average time spent in state k by time t if the system started from state h. Because the state space Ω includes some absorbing states, then the average time spent in those states by time t will diverge as $t \to +\infty$.

4.2 Households model

Different disease histories in different environments can be modelled using different recovery rates. However, because of the artificiality of such an assumption, we refrain from doing so and denote the unique recovery rate with ν. Instead, we distinguish between the within-households one-to-all infectious contact rate β_h and the global infectious contact rate β_g.

When the infectivity profile of a household of size n_H is considered, it is convenient to include among the possible states of the household only those ones where there is at least one infective. We therefore consider the state space Ω_H of the transient states only. We define Q_H as $Q_H = \Sigma - \Delta$, where Σ is the generator matrix of the CMTC on the transient states only (computed from the rates $\lambda_h = \beta_h/(n_H - 1)$ and ν) and Δ is a diagonal "death" matrix ("death" in the sense of ending the household infectious life), with diagonal elements given by $\nu i_k, k = 1, \ldots |\Omega_H| = n_H(n_H + 1)/2$. From Q_H it is then possible to obtain the matrix $P^H(\tau_H) = \mathrm{e}^{\tau_H Q_H}$ giving the probability that the system is in each states at time τ_H after having started from each possible state and, in turn, the matrix $M^H(\tau_H) = \int_0^{\tau_H} P(\sigma)\mathrm{d}\sigma$. Because the absorbing states are excluded from the computation, it is also informative to consider the limit of $M^H(\tau_H)$, as $\tau_H \to +\infty$. It is possible to prove (see Diekmann and Heesterbeek 2000, pp. 105–106) that the fact that the integral in $M^H(\tau_H)$ converges as $\tau_H \to +\infty$ is equivalent to Q_H being invertible and that

$$M^H := \lim_{\tau_H \to +\infty} M^H(\tau_H) = -{Q_H}^{-1}.$$

Each element m^H_{hk} of M^H therefore describes the average time spent in state k if the household epidemic started from state h, throughout the entire household epidemic. (A formal proof of Q_H being invertible requires noting that Q_H is strictly diagonally dominant with negative diagonal elements and invoking Gershgorin's circle theorem to conclude that the spectral bound of Q_H (i.e. the $\sup\{\mathrm{Re}(\vartheta) : \vartheta$ is an eigenvalue of $Q_H\}$) is negative.)

Since the one-to-all rate of global infections when the system is in state k is given by $\beta_g i_k$, the total global infectivity of the household can be easily computed by summing across all states:

$$R_* = \sum_{k=1}^{|\Omega_H|} \beta_g i_k (-Q_H^{-1})_{1k},$$

where the row index 1 is fixed because the state $k = 1$, corresponding to $(X, Y) = (n - 1, 1)$, is the one from which a household starts when infected from outside.

A similar approach can be used when the real-time growth rate r is studied. The infectious profile of the household at time τ_H after its infection is given by

$$\beta_H(\tau_H) = \sum_k \beta_g i_k P^H_{1k}(\tau_H) = \sum_k \beta_g i_k (e^{Q_H \tau_H})_{1k}.$$

The real-time growth rate r is such that $L_{\beta_H}(r) = 1$, where now

$$\begin{aligned} L_{\beta_H}(r) &= \int_0^{+\infty} \beta_H(\tau_H)\, \mathrm{e}^{-r\tau_H}\, \mathrm{d}\tau_H \\ &= \sum_k \beta_g i_k \int_0^{+\infty} \left(\mathrm{e}^{Q_H \tau_H}\right)_{1k} \mathrm{e}^{-r\tau_H}\, \mathrm{d}\tau_H \\ &= \sum_k \beta_g i_k \int_0^{+\infty} \left(\mathrm{e}^{Q_H \tau_H}\, \mathrm{e}^{-rJ\tau_H}\right)_{1k} \mathrm{d}\tau_H \\ &= \sum_k \beta_g i_k \left(-(Q_H - rJ)^{-1}\right)_{1k}, \end{aligned}$$

where J represents the identity matrix and it has been used for $e^{-rJ\tau}$ the fact that for the exponential of a diagonal matrix with diagonal elements δ_i is a diagonal matrix with diagonal elements e^{δ_i}, $i = 1, \ldots, |\Omega_H|$.

An iterative method can now be used to solve Eq. (4) for r (the solution exists and is unique). Each step requires only that a matrix is inverted, instead of the inefficient computation of integrals and matrix exponentials.

4.3 Households–workplaces model

Extending the methodology to the model with households and workplaces requires not only the rate of global infections, but also the rates γ_H and γ_W at which new cases appear in households and workplaces. For this reason, consider again a single small population and focus on the rate at which a new case occurs. The rate at time t at which the system reaches state (i_k, j_k) because of an infection event is given by

$$\lambda(i_k + 1)(j_k - 1)\, p_{\kappa_n(i_k+1, j_k-1)}(t),$$

where $p_{\kappa_n(i_k+1, j_k-1)}(t)$ represents the probability that at time t there is one susceptible more and one infective less than what required and this quantity is multiplied by the rate of occurrence of an infection.

Extend the notation of the previous section in the natural way, defining τ_W, λ_w, Q_W, P^W and M^W, respectively, as the time since the infection of the workplace, the one-to-one within-workplace infectious contact rate, the (defective) generator matrix for the transient states in the workplace epidemic, the probability of being and the average time spent in each state of the workplace epidemic, having started from each possible state. Then, γ_H is constructed as

$$\gamma_H(\tau_H) = \sum_k \lambda_h s_k i_k\, p^H_{1k}(\tau_H),$$

and an analogous definition holds for γ_W.

Each element of the operator K_r defined in (6) needs to be computed. The elements containing β_{GG} and β_{GL} do not need particular attention as their construction is the same as in the case of the households model. The term containing β_{LL} is elaborated as

$$\begin{aligned}
&\int_0^{+\infty} \beta_{LL}(\tau_H)\,\mathrm{e}^{-r\tau_H}\,\mathrm{d}\tau_H = \int_0^{+\infty} \gamma_H * \gamma_W(\tau_H)\,\mathrm{e}^{-r\tau_H}\,\mathrm{d}\tau_H \\
&= \left[\int_0^{+\infty} \gamma_H(\tau_H)\,\mathrm{e}^{-r\tau_H}\,\mathrm{d}\tau_H\right]\left[\int_0^{+\infty} \gamma_W(\tau_W)\,\mathrm{e}^{-r\tau_W}\,\mathrm{d}\tau_W\right] \\
&= \left[\int_0^{+\infty} \left(\sum_h \lambda_h s_h i_h P_{1h}^H(\tau_H)\right)\mathrm{e}^{-r\tau_H}\,\mathrm{d}\tau_H\right]\left[\int_0^{+\infty} \left(\sum_k \lambda_w s_k i_k P_{1k}^W(\tau_W)\right)\mathrm{e}^{-r\tau_W}\,\mathrm{d}\tau_W\right] \\
&= \left[\sum_h \lambda_h s_h i_h \left(\int_0^{+\infty} \mathrm{e}^{(Q_H - rJ)\tau_H}\,\mathrm{d}\tau_H\right)_{1h}\right]\left[\sum_k \lambda_w s_k i_k \left(\int_0^{+\infty} \mathrm{e}^{(Q_W - rJ)\tau_W}\,\mathrm{d}\tau_W\right)_{1k}\right] \\
&= \left[\sum_h \lambda_h s_h i_h \left((rJ - Q_H)^{-1}\right)_{1h}\right]\left[\sum_k \lambda_w s_k i_k \left((rJ - Q_W)^{-1}\right)_{1k}\right].
\end{aligned}$$

The second line follows from the first because of Laplace transform properties.

The term containing β_{GL} simply needs the additional contribution of another workplace epidemic (see Sec. 2.2 or Pellis et al. 2009):

$$\begin{aligned}
\int_0^{+\infty} \beta_{LG}(\tau_H) e^{-r\tau_H}\mathrm{d}\tau_H = &\left[1 + \sum_h \lambda_h s_h i_h \left((rJ - Q_H)^{-1}\right)_{1h}\right] \\
&\times \left[\sum_k \lambda_w s_k i_k \left((rJ - Q_W)^{-1}\right)_{1k}\right].
\end{aligned}$$

Finally, the implicit Eq. (7) is solved iteratively for r.

This numerical technique is exact and efficient. However, we refrain from presenting computations performed with it. We proceed instead in describing an approximate technique for the computation of r for the TVI model, which is then used for numerical results and for the application presented in Sect. 6. The reason for this choice is twofold: first, because the technique described above is exact, while the methods for the TVI model requires numerical tests to asses the quality of the approximation; second, because the natural assumption that in the TVI model the infectivity starts from zero and gradually builds up as time-since-infection progresses leads to usually lower and more realistic values of r with respect to the sSIR model, for which an individual is infectious immediately after infection. Of course, more realistic growth rates would be obtained also with the sSIR model, if a latent period were added.

5 Approximate dynamics for the non-Markovian case

5.1 Approximate epidemic dynamics in a small population

The exact dynamics obtained in the previous section are limited to the Markovian case. However, for models characterised by a non-random time-varying infectivity profile, an approximate method for dealing with the otherwise intractable dynamics has been originally proposed by Fraser (2007) for the households model. The method is embedded in the present formalism and extended to the model with households and workplaces and to a random disease history, conditional on Assumption (A.3) being satisfied. Note that, because the Markovian model violates Assumption (A.3), the following method is not a generalisation of that presented in Sect. 4, but rather complements it. For the sake of simplicity and in order to facilitate the comparison with Fraser (2007), the method will be here exposed for a non-random TVI disease history. A few comments about its extension to the random case are reported at the end of this section and some computations with the extended model are performed at the end of Appendix E.

Because in a small population repeated infectious contacts occur towards the same individual and only the first one results in an infection, the rate at which the second case is infected should take into account the probability of the initial susceptible avoiding the infection over time (*surviving probability*). The idea proposed by Fraser (2007) is to compute the average number of cases in each generation using the Reed-Frost model and to assume that each generation infects the cases in the following generation with time distribution given by $\omega(\tau)$, thus ignoring the contribution of the surviving probability, i.e. ignoring the presence of repeated infectious contacts between the same individuals. Therefore, given that the initial infective constitutes generation 1, generation 2 contains an average of μ_2 cases, which occur at times distributed as $\omega(\tau)$, generation 3 contains an average of μ_3 cases, which occur at times distributed as $\omega^{[2]}(\tau) = \omega * \omega(\tau)$, and so on. Here, $\omega^{[i]}(\tau)$ represents the i-th autoconvolution of ω, with $\omega^{[1]} = \omega$, and μ_i represents the average number of cases in generation i, computed using the Reed-Frost model. The maximum number of generations is n.

Note that, in addition to ignoring repeated infectious contacts between the same individuals, the method ignores the fact that generations can overlap, when an individual counted in generation i in the Reed-Frost model is actually infected by other cases belonging to later generations. In the terminology of Ludwig (1975), this means that the real-time generation of each individual is approximated by his or her rank, and therefore that real cases tend to occur somewhat earlier than what is described by the approximation (e.g. see Figure 2 of Fraser 2007).

In summary, the overall average rate $\gamma(\tau)$ at which new cases appear in the population is approximated by

$$\gamma_{max}(\tau) = \sum_{i=2}^{n} \mu_i \omega^{[i-1]}(\tau). \tag{9}$$

Both elements involved in the approximation, namely neglecting overlapping generations and repeated infectious contacts between the same individuals, cause the

approximation to overestimate the time of occurrence of new cases. In order to bracket the shape of $\gamma(\tau)$ between two analytically tractable approximations, Fraser (2007) suggested an underestimation obtained by lumping all cases, except from the initial one, in the second generation. This gives rise to the other approximation:

$$\gamma_{min}(\tau) = \mu\omega(\tau), \tag{10}$$

where $\mu = \sum_{i=2}^{n} \mu_i$ represents the average number of initial susceptibles who are ultimately infected. The rate γ_{min} does not represent a true lower bound approximation in general, as it still ignores the effect of overlapping generations and repeated infectious contacts. In fact, in the extreme case of 2 individuals $\gamma_{min} = \gamma_{max}$. Most of the time, however, the rate γ_{min} underestimates the times of infection of new cases, thus giving rise to a faster epidemic but with the same final size $1 + \mu$. As discussed later on, we consider Eq. (9) as our main approximation, and we use it for the details in the following sections. A numerical investigation of how close it is to the exact rate $\gamma(\tau)$ is reported in Appendix E.

Extensions to random total infectivities require computing the μ_i's from a randomised version of the Reed-Frost model, instead of the standard one [see for example Picard and Lefèvre (1990) for efficient computational techniques]. When a random infectious contact time distribution is considered, the same calculations performed before hold for $\omega(\tau)$ defined as the (pointwise) average of the infectious contact time distributions, thanks to the linearity of the convolution operation. However, as discussed in Sect. 2.3, if both the total infectivity and the infectious contact time distribution are random, we require them to be independent of one another within the same individual (Assumption (A.3)).

5.2 Households model

In the households model, with the notation introduced in Sect. 2.2, the approximate infectiousness profile of a household of size n_H obtained using (9) is

$$\begin{aligned}\beta_H(\tau_H) &= \beta_g(\tau_H) + \beta_g * \gamma_H(\tau_H) \\ &\approx R_g\omega_g(\tau_H) + R_g\omega_g * \left(\sum_{i=2}^{n_H} \mu_i^H \omega_h^{[i-1]}\right)(\tau_H).\end{aligned} \tag{11}$$

From Eq. (4), the real-time growth rate r is then approximated by the implicit solution of

$$1 = R_g \left(\int_0^{+\infty} \omega_g(\tau_H)\, \mathrm{e}^{-r\tau_H}\, \mathrm{d}\tau_H\right) + \sum_{i=2}^{n_H} \mu_i^H \left(\int_0^{+\infty} \omega_h^{[i-1]}(\tau_H)\, \mathrm{e}^{-r\tau_H}\, \mathrm{d}\tau_H\right).$$

A simplification is obtained by following Fraser (2007) and defining

$$\int_0^{+\infty} \omega_g(\tau) e^{-r\tau} \mathrm{d}\tau = \frac{1}{S_g}, \qquad \int_0^{+\infty} \omega_h(\tau) e^{-r\tau} \mathrm{d}\tau = \frac{1}{S_h}.$$

Here S_g represents the basic reproduction number that would be related to r if the households structure were ignored. Laplace transform properties imply that

$$\int_0^{+\infty} \omega_h^{[i-1]}(\tau_H)\, \mathrm{e}^{-r\tau_H}\, \mathrm{d}\tau = \left(\int_0^{+\infty} \omega_h(\tau)\, \mathrm{e}^{-r\tau}\, \mathrm{d}\tau \right)^{i-1} = \frac{1}{S_h^{i-1}}.$$

Therefore, the approximate real-time growth rate for the households model is given by the equation

$$\frac{R_g}{S_g} \left(1 + \sum_{i=2}^{n_H} \frac{\mu_i^H}{S_h^{i-1}} \right) = 1. \tag{12}$$

In the particular case of $\omega_h = \omega_g = \omega$, because $\mu_1 = 1$ and $\omega^{[1]} = \omega$, then the approximate household infectivity profile given in Eq. (11) simplifies to

$$\beta_H(\tau_H) = R_g \sum_{i=1}^{n_H} \mu_i^H \omega^{[i]}(\tau_H)$$

and Eq. (12) becomes

$$R_g \sum_{i=1}^{n_H} \frac{\mu_i^H}{S^i} = 1,$$

where now $S = (\int_0^{+\infty} \omega(\tau) e^{-r\tau} \mathrm{d}\tau)^{-1}$.

5.3 Households–workplaces model

Consider the households–workplaces model and assume, for the time being, that all households and all workplaces have the same sizes n_H and n_W, respectively. The real-time growth rate is then obtained by requiring that the operator (6) have dominant eigenvalue 1.

With the same construction as before, the following approximations hold:

$$\gamma_H(\tau_H) \approx \sum_{i=2}^{n_H} \mu_i^H \omega_h^{[i-1]}(\tau_H)$$
$$\gamma_W(\tau_W) \approx \sum_{j=2}^{n_W} \mu_j^W \omega_w^{[j-1]}(\tau_W),$$

where μ_i^H and μ_j^W represent the average numbers of cases in generation i in a Reed-Frost model for a household epidemic and in generation j in a Reed-Frost model for a workplace epidemic, respectively.

The elements of (6) involving only households epidemics and global infectious contacts are approximated in the same fashion as for the households model. The "LL" element of K_r is given by:

$$\int_0^{+\infty} \beta_{LL}(\tau_H) e^{-r\tau_H} d\tau_H = \int_0^{+\infty} \gamma_W * \gamma_H(\tau_H) e^{-r\tau_H} d\tau_H$$
$$\approx \left(\sum_{i=2}^{n_H} \mu_i^H \int_0^{+\infty} \omega_h^{[i-1]}(\tau_H) e^{-r\tau_H} d\tau_H \right) \left(\sum_{j=2}^{n_W} \mu_j^W \int_0^{+\infty} \omega_w^{[j-1]}(\tau_W) e^{-r\tau_W} d\tau_W \right).$$

Adding to S_g and S_h, as defined for the households model, also

$$S_w = \left(\int_0^{+\infty} \omega_w(\tau) e^{-r\tau} d\tau \right)^{-1},$$

the "LL" term simplifies to

$$\int_0^{+\infty} \beta_{LL}(\tau_H) e^{-r\tau_H} d\tau_H \approx \left(\sum_{i=2}^{n_H} \frac{\mu_i^H}{S_h^{i-1}} \right) \left(\sum_{j=2}^{n_W} \frac{\mu_j^W}{S_w^{j-1}} \right).$$

With similar arguments, and recalling that, when a case infected globally, the epidemics in the household and the workplace start simultaneously and therefore $\tau_H = \tau_W$,

$$\int_0^{+\infty} \beta_{LG}(\tau_H) e^{-r\tau_H} d\tau_H = \int_0^{+\infty} \left(\gamma_W(\tau_H) + \gamma_W * \gamma_H(\tau_H) \right) e^{-r\tau_H} d\tau_H$$
$$\approx \left(1 + \sum_{i=2}^{n_H} \frac{\mu_i^H}{S_h^{i-1}} \right) \left(\sum_{j=2}^{n_W} \frac{\mu_j^W}{S_w^{j-1}} \right),$$

Therefore

$$K_r \approx \widetilde{K_r} = \begin{pmatrix} \left(\sum_{i=2}^{n_H} \frac{\mu_i^H}{S_h^{i-1}}\right)\left(\sum_{j=2}^{n_W} \frac{\mu_j^W}{S_w^{j-1}}\right) & \left(1+\sum_{i=2}^{n_H} \frac{\mu_i^H}{S_h^{i-1}}\right)\left(\sum_{j=2}^{n_W} \frac{\mu_j^W}{S_w^{j-1}}\right) \\ \frac{R_g}{S_g}\left(1+\sum_{i=2}^{n_H} \frac{\mu_i^H}{S_h^{i-1}}\right) & \frac{R_g}{S_g}\left(1+\sum_{i=2}^{n_H} \frac{\mu_i^H}{S_h^{i-1}}\right) \end{pmatrix} \tag{13}$$

from which the approximate value of r can be computed numerically as the solution of $\rho(\widetilde{K_r}) = 1$.

6 Application to influenza

6.1 Derivation of R_H from the growth rate

Fraser (2007) inverted the methodology presented above for the household model in order to derive the value of the household reproduction number R_* for influenza. Here we extend those results to the case of the households–workplaces model, with the purpose of estimating the household reproduction number R_H from the real-time growth rate r. To facilitate quantitative comparison, we maintain consistency with the parameters in Fraser (2007) concerning households. The lack of information about workplace size distribution and the limited data about workplace transmission will be reflected in a range of possible values for R_H.

Although this is not a requirement of our method, in order to facilitate comparison with Fraser (2007) we use the same infectious contact time distribution $\omega(\tau)$ for all environments. We assume that r is observed from data and that $\omega(\tau)$ and the within-household and within-workplace infectious contact reproduction numbers are known (together with the household and workplace size distributions): the only unknown in the matrix K_r defined in (13) is R_g. Requiring that $\rho(K_r) = 1$ gives an implicit condition for R_g, which satisfies the following:

Theorem 2 *For $\widetilde{K_r}$ as defined in (13), the solution $\overline{R_g}$ of the equation $\rho(\widetilde{K_r}(R_g)) = 1$ exists and is unique. In addition, $\overline{R_g}$ is strictly positive if and only if*

$$\left(\sum_{i=2}^{n_H} \frac{\mu_i^H}{S^{i-1}}\right)\left(\sum_{j=2}^{n_W} \frac{\mu_j^W}{S^{j-1}}\right) < 1. \tag{14}$$

The proof is reported in Appendix D.

If condition (14) is not satisfied, the solution $\overline{R_g}$ is negative and therefore not acceptable. This reflects the fact that not all values of r are compatible with the assumptions concerning within-household and within-workplace infectivities (and the household and workplace sizes). In fact, similarly to the fact that $r > 0 \Leftrightarrow R_0 > 1$ in a homogeneously mixing population (as shown in Diekmann et al. 2010), we have here that $r > 0 \Leftrightarrow R_H > 1$. Assume now that $R_g = 0$: then $R_H = \mu_H \mu_W = \rho(\widetilde{K_0}(0))$. For a sufficiently strong infectivity in households and workplaces, $R_H > 1$ even if there

is no global transmission (this is the case when the average clump size is infinite). Because $r > 0 \iff R_H > 1$, in this case $\rho(\widetilde{K_r}(0)) = 1$ is solved by a positive value of r, which represents a lower bound under which no value of r can correspond to a positive value of $\overline{R_g}$.

The procedure just described cannot be expressed in a closed formula as nicely as in Fraser (2007), where the particularly simple expression of R_* for the households model allows its direct computation without requiring an intermediate value for R_g, which cancels out from the main formula.

Neglecting the effects of repeated infectious contacts between the same individuals and of overlapping generations results in an overestimation of R_H. The underestimation described above, where all non-primary cases in a local epidemic are lumped in the second generation, allowed Fraser (2007) to bracket the value of R_* into a small interval, thus making the method highly predictive. The same approach, however, is expected to give a worse performance in the case of the household-workplaces model for two main reasons: first, chaining two local epidemics where all non-primary cases are lumped in the second generation is worse than doing it only once; second, a workplace (e.g. a class) can be larger than a household, and thus the average final size can be much larger too: therefore, placing all cases in the second generation leads to dramatically different dynamics, much more than what would occur for a smaller local structure, as it is the case for a household.

However, Fraser (2007) showed that, in the case of influenza, the upper approximation is much closer to the exact value than the lower bound, because influenza is not particularly infectious. For this reason, and because the lower bound obtained with this method is excessively low, it is arguably not worth bracketing the solution between two bounds and accept instead the upper bound as the approximate result. Although such a decision is not completely satisfying, it must be noted that: (i) more precise results would still be only indicative, given the lack of information concerning workplace transmission, and (ii) the large local structures, which are responsible for an excessively low lower bound, have at the same time the effect of weakening the saturation effects (repeated infectious contacts between the same infector and infectee are rare) and therefore making the approximation more accurate.

Finally, although the lack of a lower bound sufficiently close to the upper bound weakens the predictive power of such an approach, nevertheless the method provides a range of reasonable values for R_H when both households and workplaces are taken into account. This is invaluable because R_H provides information about how much between-household transmission needs to be blocked in order to stop an epidemic, and not only there are no estimates of R_H in the literature, when households and workplaces are taken into account, but there is even no intuitive range of possible values for it.

6.2 Numerical results

Any possible application of this method to a practical example is likely to be very artificial, given the lack of data concerning workplaces. Some data are available about schools, though, and it is reasonable to assume that classes are larger than workplaces

(interpreted as small groups, e.g. offices, for which homogeneous mixing can be assumed) and infectious contact rates between children are larger than between adults.

Possible numerical values of transmission rates for influenza in schools are obtained from Cauchemez et al. (2008): the authors assume a disease history of type TVI with the form $\beta(\tau) = \beta f(\tau)/n$, where $f(\tau)$ is the survival function of the a *gamma* distribution with mean $\mu = 3.8$ days and a standard deviation of $\sigma = 2.0$ days (obtained from Cauchemez et al. 2004, to which they refer), n is the size of the workplaces and values of β are estimated in different conditions in Table SI5 and Table SI10 of Cauchemez et al. (2008) to be 0.22 and 0.28 day^{-1}. Since in Cauchemez et al. (2004) the average duration of the infectious period is assumed to be of 3.8 days, these values correspond roughly to $C_w = 0.84$ and $C_w = 1.1$, respectively. The disease history is taken from Fraser (2007) to be of type TVI, where all individuals have the same infectivity profile characterised by an infectious contact time distribution $\omega(\tau)$ that follows a $\Gamma(\alpha, \delta)$ distribution with $\alpha = 9.39$ and $\delta = 3.29$ (mean 2.85 and standard deviation 0.93). These values are here approximated to $\alpha \approx 9$ and $\delta \approx 3.16$, so that α is integer and the generation time T_g is fixed to 2.85 days. The size distribution of households and the within-household infectivity are again taken according to the influenza data presented in Fraser (2007): the household size distribution is that of the UK census data (2001) and $C_h = 1.35$: the average epidemic size in the household of a randomly selected individual including the primary case $(1 + \mu_H)$ is then equal to 1.87.

Further assumptions are unavoidably strong:

1. The "workplace" of a child is the class, where homogeneous mixing can be reasonably assumed, and not the entire school.
2. However, estimated transmission rates in schools are assumed for the transmission in classes.
3. Classes are taken to be of 20 students: although they could be larger, given the illustrative purpose of this numerical example, we refrain from using too large groups, for which the computation of the generations of infectives in the Reed-Frost model can become numerically challenging.
4. Roughly 20% of the population goes to school and the other 80% to workplaces (according to the UK National Statistics 2005, roughly 10 million individuals in the UK are less than 16 years old, out of a total population of 50 millions).
5. The same one-to-all transmission rate in schools occurs also in workplaces.
6. A lower bound for the effective workplace size is obtained when $n_W = 1$, i.e. there is no pure workplace transmission but only school transmission. Note that in this case, since there is no pure workplace transmission, R_g is expected to be higher than if $n_W > 1$, since it effectively contains also the transmission that is likely to occur at work.
7. Another possible value for the workplace size is arbitrarily taken to be $n_W = 4$ (we have in mind small offices).

Figures 2, 3 and 4 show the approximate values of R_H as a function of r computed using a MatLab built-in iterative method (the function *fzero*). In all figures, the top line represents the main approximation and the bottom line the less useful lower bound described before. The crosses represents the output of the stochastic simulation for

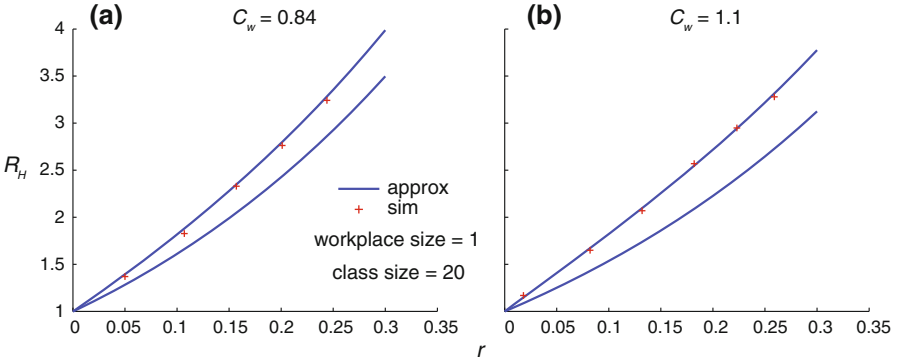

Fig. 2 The household reproduction number R_H as a function of the real-time growth rate r, obtained when 20% of the population (children) go to workplaces of size 20 (school classes) and the remaining 80% (adults) go to workplaces of size 1. The *two lines* represent the main approximation described in the text (*top*) and the lower bound approximation obtained by lumping all non-primary cases in the second generation (*bottom*). The *crosses* are the result of the individual-based stochastic simulation. The household size distribution is obtained from the UK census data (2001) and the within households infectivity is given by $C_h = 1.35$. In **a**, $C_w = 0.84$ and the simulation results are obtained, for increasing r, for values of R_g of 0.4, 0.6, 0.8, 1 and 1.2; in **b**, $C_w = 1.1$ and the simulation results are obtained, for increasing r, for values of R_g of 0.2, 0.4, 0.6, 0.8, 1 and 1.2

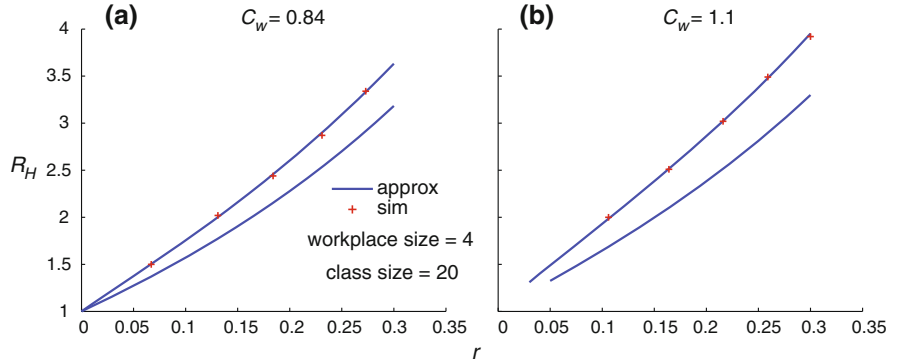

Fig. 3 The household reproduction number R_H as a function of the real-time growth rate r, for $C_w = 0.84$ (**a**) and $C_w = 1.1$ (**b**), obtained when 20% of the population (children) go to workplaces of size 20 (school classes) and the remaining 80% (adults) go to workplaces of size 4. The *two lines* represent the main approximation described in the text (*top*) and the lower bound approximation (*bottom*). The *crosses* are the result of the individual-based stochastic simulation and are obtained, for increasing r, for values of R_g of 0.2, 0.4, 0.6, 0.8 and 1 in both cases. Note that r cannot decrease below a certain level, given that $R_g \geq 0$ (see *text*)

different values of R_g. The plotted results are computed by running 100 epidemic realisations in a population of a million individuals (refer to Pellis 2009, PhD thesis, Section 6.1, for details about the simulation). The numerical estimation of R_H from simulation outputs is not straightforward, and is not a primary concern of this study. We thus used an ad hoc method based on summing the contribution of all large epidemics and computing R_H as a time-varying average of the number of households

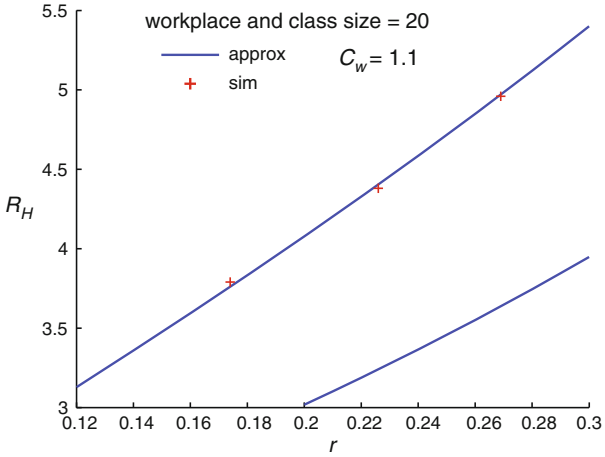

Fig. 4 The household reproduction number R_H as a function of the real-time growth rate r, for $C_w = 1.1$, obtained when all workplaces have size 20 (population of children). The *two lines* represent the main approximation described in the text (*top*) and the lower bound approximation (*bottom*). The *crosses* are the result of the individual-based stochastic simulation and are obtained, for increasing r, for values of R_g of 0.2, 0.4 and 0.6. The household size distribution is obtained from the UK census data (2001) and the within households infectivity is given by $C_h = 1.35$ (see *text*). Note the limited predictive power of the method due to presence of many large workplaces

infected by a single household. We then recorded its (theoretically constant) value during the exponentially growing phase, as assessed by visual inspection. No standard deviation is therefore associated with the point estimates. Though this ad hoc method could obviously be improved and systematised, close consistency of these estimates with theoretical expectations suggest that the method is quite accurate. Note that, in all figures, the main approximation is an upper bound, but it may not always appear so because of the closeness to the exact result and the limited accuracy in reading the value of R_H during the exponentially growing phase.

In Fig. 2a, C_w is taken to be 0.84, while in Fig. 2b, $C_w = 1.1$. In both cases school classes have size 20 and workplaces have size 1, i.e. adults transmit only via global infections. From Fig. 2a, a real time growth rate $r = 0.2\text{days}^{-1}$ for influenza as considered in Fraser (2007) gives a value of $R_H = 2.49$ and a corresponding value of $R_g = 1.1$ out of an R_0 of 1.74 (from Fraser 2007; the additional presence of workplaces does not alter R_0 significantly: not shown, refer to Pellis 2009, PhD thesis, Section 6.2.4, for more details), i.e. global infections count for more than 60% of the total transmission of an infective. From Fig. 2b, the same $r = 0.2\text{days}^{-1}$ leads to $R_H = 2.71$ and $R_g = 0.9$ out of the same value of R_0 (the same r corresponds to very similar values of R_0 for the TVI disease history; not shown, see Pellis 2009, PhD thesis, Section 6.2.4, for details), giving a contribution of the global infections to R_0 of more than 50%.

Figure 3 reports the same analysis in the case of workplaces of size 4, for the same values of C_w used before. For $r = 0.2$ days^{-1}, the values of R_H obtained in Fig. 3a, b are, respectively, $R_H = 2.60$ and $R_H = 2.86$, with corresponding values of R_g

of 0.71 and 0.54, i.e. of 40% and less than 30% of the same $R_0 = 1.74$. Separating the transmission out of school in workplace and pure community transmission, apart from substantially decreasing R_g as expected, associates to the same r larger values of R_H.

As an extreme case and to show how the lower approximation can be become hardly informative to be useful in the cases of large workplaces, the same analysis as before is reported in Fig. 4 for $C_w = 1.1$ and assuming a full population of children, i.e. in which all individuals have workplaces of size 20 with school-like transmission rates. For $r = 0.2$ days^{-1}, a value of $R_H = 4.1$ is obtained, and $R_g = 0.35$ represents only 20% of the total transmission of an infective.

These numerical results all lead to household reproduction numbers, related to a real-time growth rate $r = 0.2\,\text{days}^{-1}$, broadly ranging from 2.5 to 2.9 for some reasonable choices of workplace sizes, and increasing to 4 for some less realistic cases. Although quantitative results have to be taken carefully, given the limited knowledge available about parameter values, they reveal rather small variations in R_H estimates even for substantial changes in the social structure. Note however how these variations result from different factors compensating for each other, as highlighted by the large differences in how much transmission occurs in the community and in workplaces for different assumptions concerning the social structure.

Finally note that, although by not much, the presence of workplaces in addition to households increases the estimates of R_H, thus warning against the risk of neglecting the complexity of the social structure when models are used to estimate the effort required to stop an epidemic.

7 Summary and conclusions

We have provided a novel and coherent methodological framework for the characterisation and the computation of the real-time growth rate for epidemic models of increasing complexity, from various forms of models with no local saturation, to models with households and workplaces.

In summary, the Lotka–Euler equation

$$\int_0^{+\infty} \beta(\tau) e^{-r\tau} \mathrm{d}\tau = 1$$

that provides an implicit condition for the real-time growth rate when a single-type model with non-random time-varying infectivity profile $\beta(\tau)$ is considered can be extended to:

1. a random infectivity profile, with average $\beta(\tau)$;
2. a random susceptibility, in addition to a random infectivity: the only difference is that $\beta(\tau)$ is now a weighted average, where the weights are given by the distribution of susceptibilities;

3. a multitype model: in this case, the Lotka–Euler equation generalises into a condition that the dominant eigenvalue of the matrix

$$K_r = \left(\int_0^{+\infty} \beta_{ij}(\tau) e^{-r\tau} \mathrm{d}\tau \right)$$

has dominant eigenvalue 1;
4. a multitype randomised model, where $\beta_{ij}(\tau)$ are now the suitable averages of the infectivity profiles between types i and j.

The assumption of separable mixing substantially simplifies the results.

When small groups are considered, as in the households or the households–workplaces models, local saturation increases dramatically the complexity of the results but, under Assumption (A.1), the global infectivity profile of a households (and similarly for workplaces) can be factorised in the form

$$\beta_H(\tau) = \beta_g(\tau) + \beta_g * \gamma_H(\tau),$$

where $\beta(\tau)$ represents the average infectivity profile of an infective outside the households and $\gamma_H(\tau)$ represents the average rate at which new cases occur in the household epidemic, i.e. the average rate at which the household cumulative incidence increases.

When both households and workplaces are considered, averaging across all random disease histories and across all possible households and workplaces epidemics, the model reduces to a two-type model (where the two types are households infected through a local workplace infectious contact and a global infectious contact, denoted by L and G) and therefore r can be obtained imposing that

$$K_r = \begin{pmatrix} \int_0^{+\infty} \beta_{LL}(\tau) e^{-r\tau} \mathrm{d}\tau & \int_0^{+\infty} \beta_{LG}(\tau) e^{-r\tau} \mathrm{d}\tau \\ \int_0^{+\infty} \beta_{GL}(\tau) e^{-r\tau} \mathrm{d}\tau & \int_0^{+\infty} \beta_{GG}(\tau) e^{-r\tau} \mathrm{d}\tau \end{pmatrix}$$

has dominant eigenvalue 1.

Numerical computation of the rate $\gamma_H(\tau)$ (respectively $\gamma_W(\tau)$) can be performed exactly in the case of Markovian processes, and has been reported here only for the simplest case of exponentially distributed length of infectious period. However, for non-Markovian models, a method proposed by Fraser (2007) to approximate the rate $\gamma_H(\tau)$ (resp. $\gamma_W(\tau)$) is described. The method is based on approximating the number of cases in each generation using a Reed-Frost model and approximating their times of occurrence by autoconvoluting the infectious contact time distribution, which describes the distribution of times between cases in subsequent generations. Numerical exploration of the quality of the approximation is reported in Appendix E, and reveals that the approximation improves with decreasing within-household infectivity and generation time distributions that are more peaked around their average.

Although applied only for an infectious contact time distribution $\omega(\tau)$ equal for all environments, the method can incorporate different infectious contact time distributions in households, workplaces and in the community, so that the infectivity profiles

in different environments are not proportional to each other. Despite a single infectious contact time distribution may be mathematically more convenient and could be reasonable in the case of mild infections, it may also be argued that an infected case is likely to spend more time outside the household at the beginning of the infectious period and much less later on, when the advent of symptoms typically forces the individual to stay at home, thus increasing the within-household infectivity and reducing the infectivity via the other routes. We have not included this feature in the application to influenza, both for consistency in the comparison with results from Fraser (2007) and because, to our knowledge, no such detailed data is available in the literature yet. However, recent data reveal that the school generation time distribution may be significantly shorter than that of other environments (Cauchemez, personal communication) and we note that this phenomenon has been included in previous studies involving large-scale individual based simulation (e.g. Ferguson et al. 2005, 2006), by assuming (even though in a slightly arbitrary way) that sick children are absent from school.

Furthermore, the method can be extended to random disease histories, by substituting the simple Reed-Frost model with a randomised one. However, in addition to independence between different individuals (Assumption (A.1)), a rather strong assumption of independence between the total infectivity and the shape of the infectivity profile within the same individual (Assumption (A.3)) is also required in order to separate the Reed-Frost model from the time component of a local epidemic as done here. Further work is needed to relax this assumption.

Even if only in the case of a non-random disease history, the application of the method to the case of influenza allows the estimation of R_H for the model with households and workplaces. Although results are not reliable from a quantitative point of view, as they are based on limited reliable data and some rather strong assumptions, they nevertheless provide some indicative numerical values for the household reproduction number R_H, ranging from 2.5 to 2.9 for educated guesses of within school transmission and arguably reasonable workplace and school sizes. A wider but safer interval of values ranges from $R_H = 2.26$, as estimated in Fraser (2007) for the pure households model, and R_H as high as 4 when the whole population mixes according to a children-like behaviour.

These values of R_H are not particularly high. Apart from being influenced by a social structure typical of developed countries (e.g. with small average household size), this is mainly caused by the relatively low infection rates of influenza in comparison to those of other infections. The additional fact that even substantial changes in the social structure lead to such moderate variations of R_H may also be characteristic of influenza and other diseases with similarly low transmission rates. Comparisons with other infections with medium (e.g. mumps) or high infection rates (e.g. measles, as done by Fraser 2007) would allow further understanding of the effective impact of social structure on disease dynamics.

Note also that the estimates obtained here for influenza do not take into account the form of assortativity in the social structure resulting from the fact that larger households tend to contain more children and therefore that school classes, which are typically much larger than offices, are preferentially connected to larger households. Since in the case of multitype models it is recognised that increasing assortative mixing between individuals is generally associated to a larger value of R_0, an increased assortative

mixing at the level of local structures may lead to an increase in the epidemic severity. However, if children living in the same household go to the same school or class, the infection is reintroduced multiple times in the same local structures thus slowing down the spread and potentially reducing the final size (in the terminology of Sect. 2.2, the network linking households and workplaces is not random, and presents many cycles of length 2). The overall effect of this assortativity is therefore unclear, and further research should focus on including it in the model by distinguishing between adults and children.

A final remark refers to how much transmission occurs in different environments. Fraser (2007) comments about the fact that UK data reveals that roughly a third of the overall transmission of an average individual occurs in the household. This justifies part of the a priori assumptions appearing in earlier studies (Ferguson et al. 2006; Wu et al. 2006) that transmission is equally partitioned between the household, the workplace and the community. The numerical examples provided here account for a contribution of global infections to the overall infectivity of an individual ranging from 20 to 60%, depending on the assumptions concerning workplaces. Note however that, because of the assumption of homogeneous mixing in each environment, we interpreted workplaces like offices or classrooms. More sophisticated rules for the interaction between individuals at work can allow the definition of workplace to change radically (a department, a school, an entire company or university), thus including as workplace transmission more and more occasional "long-range" infections and reducing substantially the contribution of global transmission. This argument highlights the fact that quantifying how much transmission occurs via different routes is more than a simple matter of parameter values which have not been estimated yet: it is problematic because of the intrinsic difficulty in defining clearly what a workplace is.

In any case, it is important to note how the method shows that the presence of workplaces in the model results in larger values of R_H compared to the simpler household model (Fraser 2007). Despite this difference being moderate in the case of influenza, it still highlights the risk of underestimating the effort required to stop the epidemic by targeting control policies at the level of households when the presence of workplaces is neglected.

Acknowledgments We gratefully acknowledge the Medical Research Council for Centre and Grant support, the Royal Society for fellowship support (CF), the EU FP7 Project FluModCont and the NIGMS MIDAS programme for research funding. We thank Prof. Frank Ball for useful discussions and ideas and the two anonymous referees for suggestions on how to improve the manuscript.

Appendix A: Factorisation of the global infectivity profile of a group

The computation of the real-time growth rate for socially structured populations heavily relies on a factorisation of the infectivity profile of a group in terms of the internal dynamics, described by the rate γ of appearance of new cases in the group and the global infectivity that each infective exerts outside the group. This section is dedicated to proving such a factorisation.

It has been noted already that, under suitable conditions, the total infectivity of a household R_* can be factorised in the form

$$R_* = R_g(1 + \mu_H),$$

where R_g represents the average global infectivity of an infected individual and μ_H represents the average number of initial susceptibles that are ultimately infected in a household epidemic started by a single initial case. The result is known as the Wald's identity for epidemics (after the general identity appearing in Wald 1947, of which it is a particular case; see Ball 1986; Andersson and Britton 2000). As highlighted in Pellis et al. (2008), it basically relies on Assumption (A.1) in the main text, i.e. on the infectious behaviour of individuals being independent of when they are infected, if infected, and who infected them (a property often referred to as *lack of correlation between infector and infectee*, see Diekmann and Heesterbeek 2000), so that the particular realisation of their disease history, if infected, can be decided before the epidemic starts. For a proof of Wald's identity for epidemics, see Ball (1986) or Andersson and Britton (2000). It relies on the same assumptions that allow the concept of generations of real infections to be substituted by Ludwig's concept of rank (Ludwig 1975; Pellis et al. 2008).

Wald's identity for epidemics concerns the total global infectivity of a household. However, for the argument proposed in this chapter, a similar result is needed for the infection rates at each point in time.

Theorem 3 *Consider a household of n individuals that mix homogeneously and consider a stochastic SIR epidemic spreading from a single initial infective. Assume that infective i makes global infectious contact with any other individual according to a Poisson process with rate $B_i^g(\tau)$ and within-household infectious contacts according to a Poisson process with rate $B_i^h(\tau)$. Assume, for each i, that $B_i^g(\tau)$ and $B_i^h(\tau)$ are independent and identical copies of the random trajectories $B_g(\tau)$ and $B_h(\tau)$, respectively, and that $B_g(\tau)$ and $B_h(\tau)$ are independent of each other. Finally, denote by $\beta_g(\tau)$ the (pointwise) average of $B_g(\tau)$ and by $\gamma_H(\tau)$ the average rate at which new household cases occur. Then, at each point in time, the global average infectivity profile of the entire household $\beta_H(\tau)$ can be factorised as*

$$\beta_H(\tau) = \beta_g(\tau) + \beta_g * \gamma_H(\tau),$$

where $*$ denotes the convolution of functions.

Proof The global contribution of the first individual does not represent a problem and can be added at the last stage. Therefore, the focus will be on the convolution term, which will be denoted by the random variable $G_H(\tau)$. Now, let U be a random vector, containing all information describing the outcome of the within-household epidemic. The interest is then focused, $\forall\tau$, on the average $\mathbb{E}_U[G_H(\tau)]$.

First, consider the case where, for every infective, $B_g(\tau)$ and $B_h(\tau)$ are non-random and equal to $\beta_g(\tau)$ and $\beta_h(\tau)$, respectively. If there are only 2 individuals in the household, then $U = (T_2)$, where T_2 represents the random time at which individual 2 is

infected. Therefore:

$$\mathbb{E}_{T_2}[G_H(\tau)] = \int_0^{+\infty} \beta_g(\tau - s_2) f_{T_2}(s_2) \mathrm{d}s_2 = \beta_g * f_{T_2}(\tau),$$

where $f_{T_2}(s_2)$ is the probability density of individual 2 getting infected at time s_2.

If there are 3 individuals, since the two initial susceptibles are indistinguishable, instead of working with the times T_2 and T_3 of infection of individuals 2 and 3, it is convenient to work with the times $T_{(2)}$ and $T_{(3)}$ at which the second and the third cases occur. Then $U = (T_{(2)}, T_{(3)})$ and, given that the joint density can be expressed as

$$f_U(s_{(2)}, s_{(3)}) = f_{T_{(3)}|T_{(2)}}(s_{(3)}|s_{(2)}) f_{T_{(2)}}(s_{(2)}),$$

at each time τ,

$$\begin{aligned}
\mathbb{E}_U[G_H(\tau)] &= \int_0^{+\infty}\int_0^{+\infty} \left[\beta_g(\tau - s_{(2)}) + \beta_g(\tau - s_{(3)})\right] f_U(s_{(2)}, s_{(3)}) \mathrm{d}s_{(2)} \mathrm{d}s_{(3)} \\
&= \int_0^{+\infty} \beta_g(\tau - s_{(2)}) f_{T_{(2)}}(s_{(2)}) \mathrm{d}s_{(2)} + \int_0^{+\infty}\int_0^{+\infty} \beta_g(\tau - s_{(3)}) \\
&\quad \times f_{T_{(3)}|T_{(2)}}(s_{(3)}|s_{(2)}) f_{T_{(2)}}(s_{(2)}) \mathrm{d}s_{(3)} \mathrm{d}s_{(2)} \\
&= \int_0^{+\infty} \beta_g(\tau - s_{(2)}) f_{T_{(2)}}(s_{(2)}) \mathrm{d}s_{(2)} + \int_0^{+\infty} \beta_g(\tau - s_{(3)}) f_{T_{(3)}}(s_{(3)}) \mathrm{d}s_{(3)} \\
&= \int_0^{+\infty} \beta_g(\tau - s) \left(f_{T_{(2)}}(s) + f_{T_{(3)}}(s)\right) \mathrm{d}s \\
&= \beta_g * \gamma_H(\tau),
\end{aligned}$$

where $f_{T_{(3)}}$ represents the marginal distribution of the third individual getting infected during the epidemic, and $\gamma_H = f_{T_{(2)}} + f_{T_{(3)}}$.

The extension to the case of n household members is straightforward, leading to

$$\gamma_H = \sum_{i=2}^{n} f_{T_{(i)}}.$$

Consider now the extension to random infectivity profiles. Let $b_i^g(\tau)$ (resp. $b_i^h(\tau)$) be a realisation of the random variable $B_i^g(\tau)$ (resp. $B_i^h(\tau)$), describing the global (resp. within-household) infectivity profile of individual i and distributed, independently for each individual, according to the random trajectory $B_g(\tau)(B_h(\tau))$ defined on a suitable space $\mathscr{B}_g$ ($\mathscr{B}_h$) with measure $\zeta_g(\zeta_h)$ and with time-point averages

$$\beta_g(\tau) = \mathbb{E}_{B_g}[B_g(\tau)] = \int\limits_{\mathscr{B}_g} b_g(\tau)\mathrm{d}\zeta_g(b_g)$$

$$\left(\beta_h(\tau) = \mathbb{E}_{B_h}[B_h(\tau)] = \int\limits_{\mathscr{B}_h} b_h(\tau)\mathrm{d}\zeta_h(b_h)\right).$$

Assume, for notational convenience, that the random variable $B_g(\tau)(B_h(\tau))$ can be expressed by a density $f_{B_g}(f_{B_h})$. This is not necessary in general.

Then, in the case of 2 individuals, $U = (B_1^h, T_2, B_2^g)$ (we ignore B_1^g, as we are not considering here the global contribution of the first case, and B_2^h, as the second case has no other susceptibles to infect). Note that, in the joint distribution

$$f_U\left(b_1^h, s_2, b_2^g\right) = f_{B_1^h}\left(b_1^h\right) f_{T_2|B_1^h}\left(s_2|b_1^h\right) f_{B_2^g|B_1^h,T_2}\left(b_2^g|b_1^h, s_2\right),$$

the factor $f_{B_2^g|B_1^h,T_2}(b_2^g|b_1^h, s_2)$ is in fact simply $f_{B_2^g}(b_2^g)$, because of the key assumption that the individuals' infectivity profiles can be drawn independently of the time of their infections and the identity (i.e. of the infectious characteristics) of their infectors. Therefore, $\forall\tau$,

$$\begin{aligned}
\mathbb{E}_U[G_H(\tau)] &= \int_0^{+\infty}\int\limits_{\mathscr{B}_g}\int\limits_{\mathscr{B}_h} b_2^g(\tau - s_2) f_{B_1^h,T_2,B_2^g}(b_1^h, s_2, b_2^g)\mathrm{d}b_1^h\mathrm{d}b_2^g\mathrm{d}s_2 \\
&= \int_0^{+\infty}\int\limits_{\mathscr{B}_g}\int\limits_{\mathscr{B}_h} b_2^g(\tau - s_2) f_{B_1^h}(b_1^h) f_{T_2|B_1^h}(s_2|b_1^h) f_{B_2^g}(b_2^g)\mathrm{d}b_1^h\mathrm{d}b_2^g\mathrm{d}s_2 \\
&= \int_0^{+\infty}\int\limits_{\mathscr{B}_g} b_2^g(\tau - s_2)\left(\int\limits_{\mathscr{B}_h} f_{T_2|B_1^h}(s_2|b_1^h) f_{B_1^h}(b_1^h)\mathrm{d}b_1^h\right) f_{B_2^g}(b_2^g)\mathrm{d}b_2^g\mathrm{d}s_2 \\
&= \int_0^{+\infty}\int\limits_{\mathscr{B}_g} b_2^g(\tau - s_2) f_{T_2}(s_2) f_{B_2^g}(b_2^g)\mathrm{d}b_2^g\mathrm{d}s_2 \\
&= \int_0^{+\infty}\left(\int\limits_{\mathscr{B}_g} b_2^g(\tau - s_2) f_{B_2^g}(b_2^g)\mathrm{d}b_2^g\right) f_{T_2}(s_2)\mathrm{d}s_2 \\
&= \int_0^{+\infty} \beta_g(\tau - s_2) f_{T_2}(s_2)\mathrm{d}s_2 \\
&= \beta_g * \gamma_H(\tau).
\end{aligned}$$

Note that, when adding the global contribution of the primary case, we have to rely on the assumptions of independence between B_1^g and B_1^h.

The extension to more than 2 individuals follows the same argument, but is omitted because of the cumbersome notation. Again,

$$\gamma_H = \sum_{i=2}^{n} f_{T_{(i)}}.$$

It is worth stressing again how such a factorisation is heavily based on the same assumptions behind Wald's identity for epidemics and Ludwig's rank-based construction (Pellis et al. 2008, 2009). □

Appendix B: Proof of Theorem 1

Proof For the sake of simplicity, consider again households all of the same size n_H. The result can be readily extended to households of variable sizes. As done in the main text, we refer to all the non-primary cases as secondary cases, independently of whether they have been infected directly or indirectly by the primary case, and we use the factorisation

$$\beta_H(\tau_H) = \beta(\tau_H) + \beta * \gamma_H(\tau_H),$$

where $\beta_g(\tau)$ is the average global infectivity profile of an individual and $\gamma_H(\tau_H)$ the average rate at which new cases appear in the household. The real-time growth rate r_H for households is given by the implicit solution of

$$L_{\beta_H}(r_H) = 1.$$

The real-time growth rate r for individuals is obtained when the two-type model with primary and secondary cases is considered. In this framework, a primary case generates other primary cases following $\beta_g(\tau) = \beta_g(\tau_H)$ (the household is infected when the primary case is infected) and secondary cases following $\gamma_H(\tau_H)$; a secondary case generates only primary cases following $\beta_g(\tau)$. For r to be the real-time growth rate for individuals, the linear operator

$$K_r = \begin{pmatrix} \int_0^{+\infty} \beta(\tau_H)\mathrm{e}^{-r\tau_H}\mathrm{d}\tau_H & \int_0^{+\infty} \beta(\tau)\mathrm{e}^{-r\tau}\mathrm{d}\tau \\ \int_0^{+\infty} \gamma_H(\tau_H)\mathrm{e}^{-r\tau_H}\mathrm{d}\tau_H & 0 \end{pmatrix} \tag{15}$$

must have dominant eigenvalue 1. A quick look at the characteristic equation (e.g. using Descartes' sign rule) reveals that the two eigenvalues have opposite signs. Imposing 1 to be an eigenvalue (which means it can only be the dominant one) implies that

$$1 - \int_0^{+\infty} \beta(\tau_H)\mathrm{e}^{-r\tau_H}\mathrm{d}\tau_H = \left(\int_0^{+\infty} \gamma_H(\tau_H)\mathrm{e}^{-r\tau_H}\mathrm{d}\tau_H\right)\left(\int_0^{+\infty} \beta(\tau)\mathrm{e}^{-r\tau}\mathrm{d}\tau\right)$$

which, by properties of the Laplace transform, can be written as

$$L[\beta + (\gamma_H * \beta)](r) = 1. \tag{16}$$

Since r and r_H are both the unique solution of the same equation (unique because the left-hand side is monotonic in r, with $\lim_{r\to+\infty} L_{\beta_H}(r) = 0$ and $L_{\beta_H}(0) = R_* > 1$: recall that we are observing a large epidemic), it follows $r = r_H$. □

Appendix C: Variable household and workplace sizes

Here we extend the results about the real-time growth rate for the households–workplaces model to the case of households and workplaces of variable sizes.

First, the rate at which a household infected either locally or globally infects another household globally does not involve workplaces and is therefore obtained by the same argument used for the households model at the end of Sect. 3.2. In the case of β_{LL} and β_{GL}, the additional presence of a workplace epidemic has to be taken into account. The notation is the following: $\pi^H_{n_H}$ and $\pi^W_{n_W}$ represents respectively the probability that a randomly selected individual belongs to a household of size n_H and a workplace of size n_W; $\gamma_H^{(n_H)}(\tau_H)$ and $\gamma_W^{(n_W)}(\tau_W)$ represent respectively the rate of appearance of new cases in a household of size n_H at time τ_H after the infection of the household and in a workplace of size n_W at time τ_W after the infection of the workplace.

Consider first the case of β_{LL}. A household of size n_H infects a workplace of size n_W at a rate $\gamma_H^{(n_H)}(\tau_H)\pi^W_{n_W}$, because the size of the workplaces where individuals living in that household work is independent of the size of the household, under the bipartite random network Assumption (A.2). Then, for the same reason, the workplace infects households of size n'_H at a rate given by $\gamma_W^{(n_W)}(\tau_W)\pi^H_{n'_H}$. By considering the contribution of each possible workplace size, a household of size n_H infected locally infects locally a household of size n'_H at an average rate of

$$\begin{aligned}\pi^H_{n'_H}\left(\sum_{n_W}\pi^W_{n_W}\gamma_H^{(n_H)} * \gamma_W^{(n_W)}(\tau_H)\right) &= \pi^H_{n'_H}\gamma_H^{(n_H)} * \left(\sum_{n_W}\pi^W_{n_W}\gamma_W^{(n_W)}\right)(\tau_H)\\ &= \pi^H_{n'_H}\gamma_H^{(n_H)} * \gamma_W(\tau_H),\end{aligned}$$

where $\gamma_W = \sum_{n_W}\pi^W_{n_W}\gamma_W^{(n_W)}$ is the average rate at which secondary cases are infected in the workplace of a randomly selected individual.

In the case of β_{LG}, consider a household of size n_H infected globally. The primary case is in a workplace of size n_W with probability $\pi^W_{n_W}$ and therefore a household of size n'_H is infected locally through this primary case at a rate

$$\pi^H_{n'_H}\sum_{n_W}\pi^W_{n_W}\gamma_W^{(n_W)}(\tau_W) = \pi^H_{n'_H}\gamma_W(\tau_H),$$

where γ_W is defined as before and $\tau_W = \tau_H$ because the two local structures are infected at the same time, i.e. the time of the infection through a global contact of the common primary case.

Any other household case is in a workplace of size n'_W with probability $\pi^W_{n'_W}$ and therefore the rate of infection of households of size n'_H through secondary cases is given, like before, by

$$\pi^H_{n'_H} \gamma_H^{(n_H)} * \left(\sum_{n_W} \pi^W_{n_W} \gamma_W^{(n_W)} \right)(\tau_H) = \pi^H_{n'_H} \gamma_H^{(n_H)} * \gamma_W(\tau_H).$$

The total rate obtained by adding the two contributions together is given by

$$\pi^H_{n'_H} \left(\gamma_W(\tau_H) + \gamma_H^{(n_H)} * \gamma_W(\tau_H) \right).$$

The real-time growth rate r is obtained by imposing a dominant eigenvalue 1 to the block operator (the index H has been dropped from the time τ_H)

$$K_r = \begin{pmatrix} \pi^H_{n'_H} \int_0^{+\infty} \gamma_H^{(n_H)} * \gamma_W(\tau) e^{-r\tau} \mathrm{d}\tau & \pi^H_{n'_H} \int_0^{+\infty} \left(\gamma_W(\tau) + \gamma_H^{(n_H)} * \gamma_W(\tau) \right) e^{-r\tau} \mathrm{d}\tau \\ \pi^H_{n'_H} \int_0^{+\infty} \left(\beta(\tau) + \gamma_H^{(n_H)} * \beta(\tau) \right) e^{-r\tau} \mathrm{d}\tau & \pi^H_{n'_H} \int_0^{+\infty} \left(\beta(\tau) + \gamma_H^{(n_H)} * \beta(\tau) \right) e^{-r\tau} \mathrm{d}\tau \end{pmatrix}$$

Note that each of the four blocks has the same dimension $N_H \times N_H$, where N_H represents the largest household size considered (assumed to be finite) and consists of a matrix with rank 1. Therefore, in general, K_r has rank 2. However, thanks to the particular structure of K_r, the computation of the dominant eigenvalue can be simplified according to the following result:

Theorem 4 *Consider m-dimensional real non-zero column vectors u, v and a, b, c, d and consider the $m \times m$ matrices*

$$A = ua^T, \quad B = ub^T, \quad C = vc^T, \quad D = vd^T,$$

where ^{T} denotes the transposition. Finally consider the $2m \times 2m$ block matrix

$$M = \begin{pmatrix} A & B \\ C & D \end{pmatrix}.$$

Then the matrix M has only 2 non-zero eigenvalues λ_1 and λ_2, which are the same eigenvalues of the 2×2 matrix

$$m = \begin{pmatrix} a^T u & b^T u \\ c^T v & d^T v \end{pmatrix},$$

whose elements are the eigenvalues of the corresponding matrices A, B, C and D. In particular, the dominant eigenvalue of M and m is the same.

Proof The proof proceeds by direct computation, based on the fact that, if λ is an eigenvalue of m with corresponding eigenvector $(x, y)^T$, $x, y \in \mathbb{R}$, then $(ux, vy)^T$ is an eigenvector of M corresponding to the same eigenvalue λ. □

Theorem 4 implies that K_r can be reduced to the two dimensional case of fixed household and workplace sizes with

$$\begin{aligned}
\beta_{LL}(\tau_H) &= \sum_{n_H} \pi_{n_H}^H \gamma_H^{(n_H)} * \gamma_W(\tau_H) \\
&= \gamma_H * \gamma_W(\tau_H) \\
\beta_{LG}(\tau_H) &= \sum_{n_H} \pi_{n_H}^H \left(\gamma_W(\tau_H) + \gamma_H^{(n_H)} * \gamma_W(\tau_H)\right) \\
&= \sum_{n_H} \pi_{n_H}^H \gamma_W(\tau_H) + \sum_{n_H} \pi_{n_H}^H \gamma_H^{(n_H)} * \gamma_W(\tau_H) \\
&= \gamma_W(\tau_H) + \gamma_H * \gamma_W(\tau_H),
\end{aligned}$$

where $\gamma_H = \sum_{n_H} \pi_{n_H}^H \gamma_H^{(n_H)}$ represents the average rate of occurrence of new cases in the household of a randomly chosen individual and the last equality holds because $\sum_{n_H} \pi_{n_H}^H = 1$.

Appendix D: Proof of Theorem 2

Proof Theorem 2 is based on the following:

Lemma 1 *Assume M is a 2-by-2 matrix of the form*

$$M = \begin{pmatrix} a & b \\ xc & xd \end{pmatrix}, \tag{17}$$

with $d > 0$, and assume that $\det M \leq 0$. *Then the dominant eigenvalue of M is an increasing function of x.*

Proof The dominant eigenvalue of M, $\rho(M)$, is given by

$$\rho(M) = \frac{1}{2}\left[(a + xd) + \sqrt{(a + xd)^2 - 4x \det M}\right].$$

The conditions $d > 0$ and $\det M \leq 0$ imply that $\rho(M)$ increases monotonically with x. □

Then, Theorem 2 follows from the fact that $\widetilde{K_r}$ of Eq. (13) has the same structure as in Lemma 1, with $R_g = x, c = d > 0$ and $b \geq a$, which implies $\det M = ad - bc = c(a - b) < 0$. Therefore $\rho(\widetilde{K_r}) = \rho(\widetilde{K_r}(R_g))$ is a continuous and monotonically increasing function of R_g. Given that $\lim_{x \to -\infty} \rho(\widetilde{K_r}(x)) = -\infty$ and

$\lim_{x\to+\infty}\rho(\widetilde{K_r}(x)) = +\infty$, the solution of $\rho(\widetilde{K_r}(R_g)) = 1$ exists and is unique. Furthermore, when $R_g = 0$,

$$\rho(\widetilde{K_r}(0)) = \left(\sum_{i=2}^{n_H}\frac{\mu_i^H}{S^{i-1}}\right)\left(\sum_{j=2}^{n_W}\frac{\mu_j^W}{S^{j-1}}\right),$$

and therefore $\overline{R_g}$ is strictly positive if and only if Condition (14) is satisfied. □

Appendix E: Numerical investigation

The main ingredient used in dealing with the real-time growth rate when local saturation effects cannot be neglected is the function γ, defined as the average rate at which a new infection occurs in a small group. It is worth analysing this function in detail.

It follows directly from its definition that, if $X(t)$ denotes the average number of susceptibles and $I_C(t)$ the average cumulative incidence of an *SIR* epidemic in a homogeneously mixing population at time t,

$$\gamma(t) = \frac{\mathrm{d}}{\mathrm{d}t}I_C(t) = -\frac{\mathrm{d}}{\mathrm{d}t}X(t). \tag{18}$$

The first equality states that the rate at which new cases appear is the same rate at which the cumulative incidence increases, which is a trivial statement (although formal details involve the exchange between the derivative and the integral defining the average across possible outcomes of the epidemic process). The second equation follows directly from the fact that the total population is constant.

This characterisation, however, is not particularly enlightening. Therefore it is worth exploring numerically this complex model component γ, and in particular the analytical approximation discussed in the main text.

Despite the approximation discussed in Sect. 5.1 does not apply to the sSIR model, because of the correlation between the infectious contact time distribution of an infective and the total infectivity (individuals that are infected for longer have higher total infectivity), the Markovian cases allow the exact dynamics to be expressed analytically. We therefore "improperly" compare the simplest case with constant recovery rate in a group of size 2 with what the approximation would lead to, even if we overlook the fact that one of the assumption at the base of the approximation is not met. In this particularly simple case, if λ denotes the one-to-one infection rate and ν the recovery rate, the average number of cases in generation 2 from the randomised Reed-Frost model is given by $\lambda/(\lambda+\nu)$, i.e. the probability that the second case is infected (*competing hazards*). The infectious contact time distribution, instead, is given by $\omega(\tau) = \nu e^{-\nu\tau}$. Therefore the approximation to the exact rate $\gamma(\tau) = \lambda e^{-(\lambda+\nu)\tau}$ would give

$$\gamma_{max}(\tau) = \frac{\lambda\nu}{\lambda+\nu}e^{-\nu\tau}. \tag{19}$$

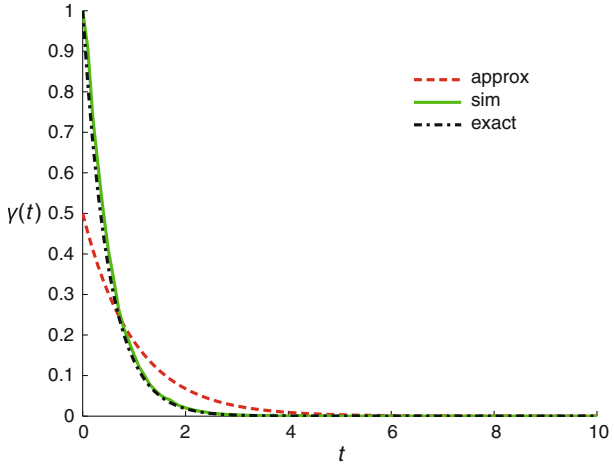

Fig. 5 Plot of the rate at which the initial susceptible in a group of size $n = 2$ acquires infection from the other case. The exact rate $\gamma(\tau)$ (*dash-dotted line*) is compared with the rate obtained by averaging across 100,000 stochastic simulations (*continuous line*) and the analytical approximation (*dashed line*) described in Eq. (19). The disease history corresponds to the Markovian case (exponentially distributed length of infectious period) with constant infectivity $\lambda = 1$ and recovery rate $\nu = 1$

As it should be, it is easily verified that

$$\int_0^{+\infty} \gamma(\tau)\mathrm{d}\tau = \int_0^{+\infty} \gamma_{max}(\tau)\mathrm{d}\tau = \frac{\lambda}{\lambda+\nu} = \mu_2 = \mu.$$

Figure 5 shows the approximation γ_{max}, together with the exact rate γ and the result of the computation of $\gamma(t) = \frac{\mathrm{d}}{\mathrm{d}t} I_C(t)$, where $I_C(t)$ is obtained by averaging across 100,000 individual-based stochastic simulations. As expected, the approximation performs poorly.

When a non-random time-varying infectivity is considered, no exact analytical result is available and therefore the comparison of the approximate rate γ_{max} is made with the average of 100,000 individual-based stochastic simulations. Figures 6 and 7 show the analytical approximation and the result of the numerical simulation for groups of size $n = 2, 5$ and 10, an average one-to-all total infectivity of $C = 1.5$ and a $\Gamma(\alpha, \delta)$-distributed infectious contact time distribution $\omega(\tau)$, with shape parameter $\alpha = 1$ (exponential), 4 and 10 and fixed generation time $T_g = \alpha/\delta = 1$. As can be seen, the approximation does not appear to improve significantly as the group size grows, but it improves considerably with increasing α, i.e. when secondary cases of an infective are more peaked around the generation time T_g.

When C within the group has value 1.5, then each individual on average makes 1.5 infectious contacts with other cases. However, when C decreases, so does the probability of repeated contacts towards the same individuals. In fact the approxima-

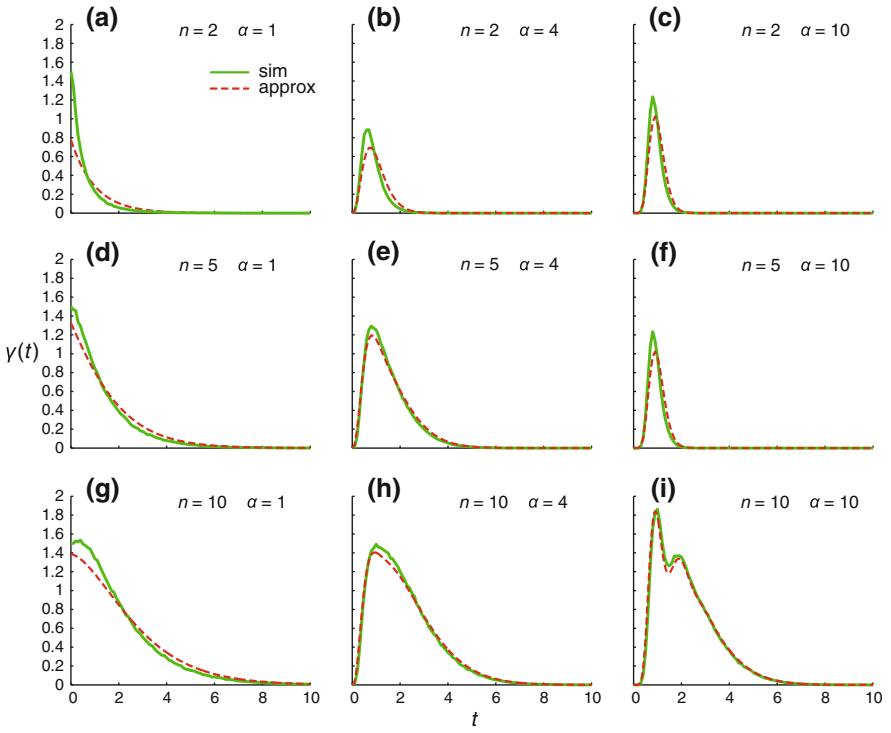

Fig. 6 Plots of the rate at which new cases occur in a local epidemic started from a single initial case. In this case, $C = 1.5$ and the infectious contact time distribution is given by $\omega(\tau) \sim \Gamma(\alpha, \delta)$ with generation time $T_g = 1$. The analytical approximation (*dashed line*) obtained from Eq. (9) is compared with the average over 100,000 stochastic simulation (*continuous line*). The group size changes by rows: from *top to bottom*, $n = 2$, 5 and 10. The shape of the infectivity profile changes by columns: from *left to right*, $\alpha = 1$ (exponential), 4 and 10. The scale parameter δ changes accordingly

tion dramatically improves as C decreases: the same situations described above are reported in Figs. 7 for $C = 0.75$.

Note however that, even when the approximation appears not to be particularly accurate, as in the case of $C = 1.5$ above, when the method is used to estimate the real-time growth rate in a structured model, the average infectious profile of the group (e.g. a household) is multiplied by e^{-rt} and therefore, for positive r, the discrepancies between the approximation and the true rate $\gamma(t)$ that occur for large t are weighted much less than those occurring for small t. Estimates of real-time growth rates are therefore more accurate when the infectious contact time distribution is Γ-distributed with shape parameter $\alpha > 1$, i.e. when the rate of appearance of new cases at the very start of the local epidemic is negligible and thus the discrepancy between the real and the approximate rate of appearance of new cases is minimal for small t (as opposed to the exponentially decaying infectivity obtained for $\alpha = 1$, see Figs. 6 and 7). Such a consideration offers an explanation that motivates the predictive power of this method highlighted in Fraser (2007).

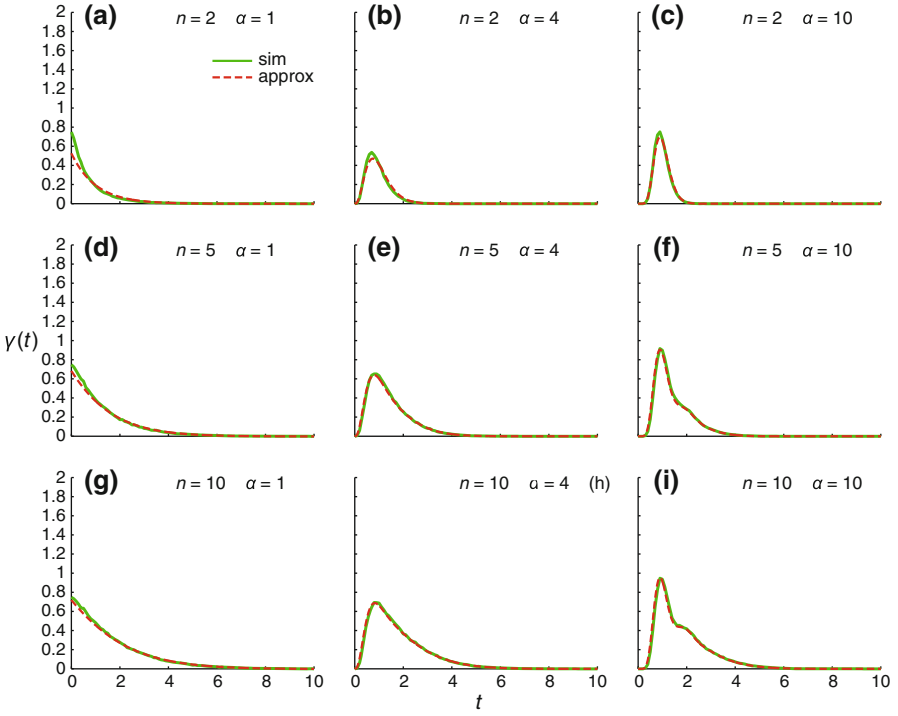

Fig. 7 Plots of the rate at which new cases occur in a local epidemic started from a single initial case. All details are the same as in Fig. 6, except that now $C = 0.75$

Finally, calculations have also been performed using a random TVI disease history (under Assumption (A.3)). Numerical computation of the average number of cases in each generation have been performed using the technique described in Picard and Lefèvre (1990) for computing the probability of observing each possible epidemic realisation from a randomised Reed-Frost model. Figure 8 reports the same output as in Fig. 6, but assuming that individuals have an exponentially distributed total infectivity with mean $C = 1.5$ and a $\Gamma(\alpha, \delta)$-distributed infectious contact time distribution $\omega(\tau)$ with values of α of 1, 4 and 10 and a mean T which is in turn randomly distributed according to a $\Gamma(\alpha', \delta')$ distribution, with $\alpha' = 4$ and mean value given by the generation time $\alpha'/\delta' = T_g = 1$. As a last example, Fig. 9 shows the rate γ_H for the same parameter choices as in Fig. 8i, but with the incorrect application of the approximation method when either (a) a simple Reed-Frost model is used instead of the randomised one (the total area under the rate γ_H is approximately 4.05 instead of the correct value of 2.93) or (b) a $\Gamma(\alpha, \delta)$-distributed infectious contact time distribution $\omega(\tau)$ with fixed mean T_g is used, instead of the pointwise average of the infectious contact time distributions with $\Gamma(\alpha', \delta')$-distributed mean T with average T_g (correct area under γ_H, but wrong shape).

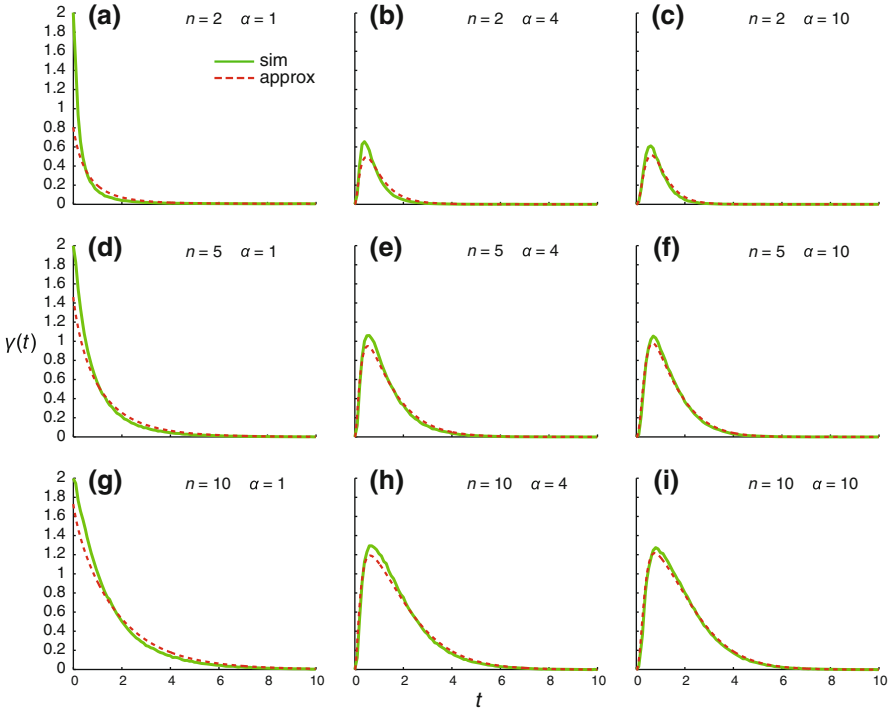

Fig. 8 Plots of the rate at which new cases occur in a local epidemic started from a single initial case. All details are the same as in Fig. 6, except for an exponentially distributed total infectivity of individuals and a Γ-shaped infectivity profile with random mean, as described in the *text*

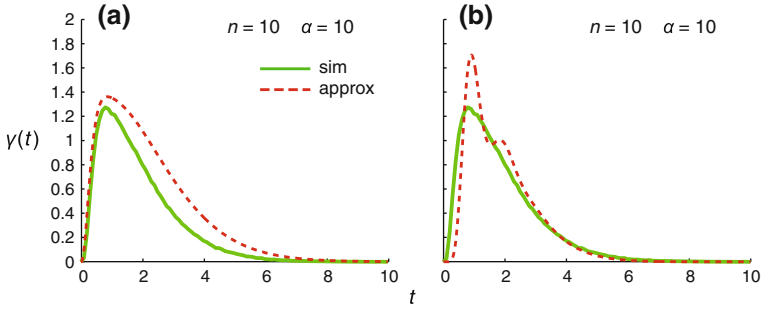

Fig. 9 Incorrect applications of the approximation method to the case of an exponentially distributed total infectivity of individuals and a Γ-shaped infectivity profile with fixed shape parameter $\alpha = 10$ and random mean, as described in the *text* (group size $n = 10$)

References

Albert R, Barabási AL (2002) Statistical mechanics of complex networks. Rev Mod Phys 74(1):47–97
Anderson RM, May RM (1991) Infectious diseases of humans: dynamics and control. Oxford University Press, Oxford

Andersson H, Britton T (2000) Stochastic epidemic models and their statistical analysis. In: Lecture notes in statistics, vol 151. Springer, New York

Ball F (1986) A unified approach to the distribution of total size and total area under the trajectory of infectives in epidemic models. Adv Appl Probab 18(2):289–310

Ball FG, Britton T (2007) An epidemic model with infector-dependent severity. Adv Appl Probab 39(4):949

Ball F, Neal P (2002) A general model for stochastic SIR epidemics with two levels of mixing. Math Biosci 180:73–102

Ball FG, Neal P (2008) Network epidemic models with two levels of mixing. Math Biosci 212(1): 69–87

Ball F, Mollison D, Scalia-Tomba G (1997) Epidemics with two levels of mixing. Ann Appl Probab 7(1): 46–89

Bansal S, Grenfell BT, Meyers LA (2007) When individual behaviour matters: homogeneous and network models in epidemiology. J R Soc Interface 4(16):879

Bartoszyński R (1972) On a certain model of an epidemic. Appl Math 13(2):139–151

Becker NG, Dietz K (1995) The effect of household distribution on transmission and control of highly infectious diseases. Math Biosci 127:207–219

Cauchemez S, Carrat F, Viboud C, Valleron AJ, Boelle PY (2004) A Bayesian MCMC approach to study transmission of influenza: application to household longitudinal data. Stat Med 23(22):3469–3487

Cauchemez S, Valleron AJ, Boelle PY, Flahault A, Ferguson NM (2008) Estimating the impact of school closure on influenza transmission from Sentinel data. Nature 452(7188):750–754

Cauchemez S, Donnelly CA, Reed C, Ghani AC, Fraser C, Kent CK, Finelli L, Ferguson NM (2009) Household transmission of 2009 pandemic influenza a (h1n1) virus in the united states. N Engl J Med 361(27):2619–2627

Colizza V, Barrat A, Barthelemy M, Valleron AJ, Vespignani A (2007) Modeling the worldwide spread of pandemic influenza: Baseline case and containment interventions. PLoS Med 4(1):e13

Diekmann O, Heesterbeek JAP (2000) Mathematical epidemiology of infectious diseases: model building, analysis and interpretation. Wiley series in mathematical and computational biology. Wiley, Chichester

Diekmann O, Heesterbeek JAP, Roberts MG (2010) The construction of next-generation matrices for compartmental epidemic models. J R Soc Interface 7(47):873–885

Edmunds WJ, O'Callaghan CJ, Nokes DJ (1997) Who mixes with whom? a method to determine the contact patterns of adults that may lead to the spread of airborne infections. Proc R Soc Lond Ser B 264(1384):949–957

Ferguson NM, Cummings DAT, Cauchemez S, Fraser C, Riley S, Meeyai A, Iamsirithaworn S, Burke DS (2005) Strategies for containing an emerging influenza pandemic in Southeast Asia. Nature 437:209–214

Ferguson NM, Cummings DAT, Fraser C, Cajka JC, Cooley PC, Burke DS (2006) Strategies for mitigating an influenza pandemic. Nature 442(7101):448

Fraser C (2007) Estimating individual and household reproduction numbers in an emerging epidemic. PLoS ONE 2(8):e758

Fraser C, Donnelly CA, Cauchemez S, Hanage WP, Van Kerkhove MD, Hollingsworth TD, Griffin J, Baggaley RF, Jenkins HE, Lyons EJ, Jombart T, Hinsley WR, Grassly NC, Balloux F, Ghani AC, Ferguson NM, Rambaut A, Pybus OG, Lopez-Gatell H, Alpuche-Aranda CM, Chapela IB, Zavala EP, Guevara DME, Checchi F, Garcia E, Hugonnet S, Roth C, Collaboration TWRPA (2009) Pandemic potential of a strain of influenza A (H1N1): early findings. Science 324(5934):1557–1561

Goldstein E, Paur K, Fraser C, Kenah E, Wallinga J, Lipsitch M (2009) Reproductive numbers, epidemic spread and control in a community of households. Math Biosci 221(1):11–25

Grassly NC, Fraser C (2008) Mathematical models of infectious disease transmission. Nat Rev Microbiol 6(6):477–487

Hethcote HW (2000) The mathematics of infectious diseases. SIAM Rev 42(4):599–653

Kendall WS, Saunders IW (1983) Epidemics in competition II: the general epidemic. J R Stat Soc Ser B 45(2):238–244

Kermack WO, McKendrick AG (1927) A contribution to the mathematical theory of epidemics. Proc R Soc Lond Ser A 115:700–721

Ludwig D (1975) Final size distributions for epidemics. Math Biosci 23:33

Neal P (2006) Multitype randomized reed-frost epidemics and epidemics upon random graphs. Ann Appl Probab 16(3):1166–1189

Newman MEJ (2003) The structure and function of complex networks. SIAM Rev 45(2):167–256

Pellis L (2009) Mathematical models for emerging infections in socially structured populations: the presence of households and workplaces. PhD thesis, Imperial College London. http://hdl.handle.net/10044/1/4696

Pellis L, Ferguson NM, Fraser C (2008) The relationship between real-time and discrete-generation models of epidemic spread. Math Biosci 216(1):63–70

Pellis L, Ferguson NM, Fraser C (2009) Threshold parameters for a model of epidemic spread among households and workplaces. J R Soc Interface 6(40):979–987

Picard P, Lefèvre C (1990) A unified analysis of the final size and severity distribution in collective Reed-Frost epidemic processes. Adv Appl Probab 22(2):269

Riley S (2007) Large-scale spatial-transmission models of infectious disease. Science 316(5829):1298–1301

Riley S, Fraser C, Donnelly CA, Ghani AC, Abu-Raddad LJ, Hedley AJ, Leung GM, Ho LM, Lam TH, Thach TQ, Chau P, Chan KP, Lo SV, Leung PY, Tsang T, Ho W, Lee KH, Lau EMC, Ferguson NM, Anderson RM (2003) Transmission dynamics of the etiological agent of sars in hong kong: Impact of public health interventions. Science 300(5627):1961–1966

Roberts M, Heesterbeek J (2007) Model-consistent estimation of the basic reproduction number from the incidence of an emerging infection. J Math Biol 55(5):803–816

Ross JV, House T, Keeling MJ (2010) Calculation of disease dynamics in a population of households. PLoS ONE 5(3):e9666

Svensson Å, Scalia-Tomba G (2001) Competing epidemics in closed populations. Research report/Mathematical Statistics, Stockholm University, 2001:8. Mathem Stat SU, Stockholm

UK census data (2001) http://www.ons.gov.uk/census/

UK National Statistics (2005) http://www.statistics.gov.uk/STATBASE/ssdataset.asp?vlnk=9390

Wald A (1947) Sequential analysis. Wiley, New York

Wallinga J, Lipsitch M (2007) How generation intervals shape the relationship between growth rates and reproductive numbers. Proc R Soc B: Biol Sci 274(1609):599–604

Wu JT, Riley S, Fraser C, Leung GM (2006) Reducing the impact of the next influenza pandemic using household-based public health interventions. PLoS Med 3(9):1532–1540

Xia Y, Bjørnstad ON, Grenfell BT (2004) Measles metapopulation dynamics: a gravity model for epidemiological coupling and dynamics. Am Nat 164(2):267–281